Chapter IV:
Tropical Pacific sub-seasonal convection

IV.1. Introduction

In this chapter I explore the relationship of westerly wind events (WWEs) to atmospheric convection as described by satellite measured outgoing longwave radiation (OLR). I compute the mean surface wind and convective structures associated with the Madden-Julian Oscillation (MJO, see Madden and Julian 1994 for a review). I examine statistical relationships that WWEs exhibit with the MJO and tropical cyclones. The work here builds on the surface wind analysis described in Chapters II and III, Harrison and Vecchi (1997, henceforth HV97) and Vecchi and Harrison (2000, henceforth VH00); and attempts to resolve the relationships that have been observed anecdotally between WWEs, the MJO and tropical cyclones.

Observations of two MJO events during the TOGA-COARE IOP suggest enhanced WWE variability associated with the MJO (Godfrey *et al.* 1998). A relationship between tropical cyclone activity and WWEs has been discussed since the first descriptions of WWEs (Keen 1982, Harrison and Giese 1991, Hartten 1996); I use the identification scheme described in Chapter II and HV97 to explore WWE relationships to the MJO and tropical cyclone activity, for the period 1986-1997. Also shown in this chapter are the results of compositing the surface wind anomaly and OLR anomaly fields for the MJO.

The Madden-Julian Oscillation (MJO; also referred to as the Intra-seasonal Oscillation or ISO) was first identified as a spectral peak in global tropical 850mb and 150mb zonal wind and wind divergence (Madden and Julian 1972) in the 40-50 day range, and has been the subject of much research by the atmospheric science community for the past 30 years. The spectral peak has been found to exist in a much broader range of 30-90 days, and is associated with globally propagating (global wavenumber 1 or 2) variability of tropo-

spheric wind and atmospheric convection (see Madden and Julian 1972, 1974, 1994, Rui and Wang 1990, Hendon and Salby 1994, Maloney and Hartmann 1998). Atmospheric convection related to the MJO is limited to the regions of warmest SST (SST>28°C) in the Indo-Pacific warm pool region, and near the Pacific Intertropical Convergence Zone (ITCZ) and South Pacific Convergence Zone (SPCZ) (see Rui and Wang 1990, Hendon and Salby 1994). The atmospheric convective structures associated with the MJO propagate eastward from the Indian Ocean at 5-10 ms^{-1} (see Rui and Wang 1990, Hendon and Salby 1994, Figures IV.5-.7); while the tropospheric zonal wind structures propagate eastward at a speed between 10 and 20 ms^{-1} (see Madden and Julian 1974,1994, Hendon and Salby 1994, Maloney and Hartmann 1998). While the free-tropospheric wind and atmospheric convection variability associated with the MJO have been previously described, the global surface wind and wind-stress anomalies associated with it merit further examination. Hendon *et al*. (1998) found that equatorial zonal wind-stress anomalies associated with the MJO extend into the central/eastern Pacific, away from the Pacific warm pool convective region.

Tropical atmospheric convection is generally associated with strong surface wind convergence; near the Equator convection usually includes surface westerlies under the convection. The period of WWE activity in Dec 1992-Jan 1993, during the TOGA/COARE IOP, which was one of the most extreme in the period 1986-1995 (see Chapter II, HV97), occurred with the passage of the convectively active phase of the MJO over the western Pacific warm pool (Lin and Johnson 1996, Chen and Houze 1996). Some of the westerly wind variability in the onset of the 1997-8 El Niño event appeared related to the MJO (McPhaden 1999). I use a quantitative definition for MJO variability developed by Maloney and Hartmann (1998, heceforth MH98) to examine MJO related surface wind and atmospheric convection variability.

There is little evidence for a systematic WWE/MJO connection in the WWE composite results described in Chapter II and HV97. None of the equatorial WWEs shows a

translation during its lifetime consistent with being a direct surface expression of the MJO (whose tropospheric with phase translates eastward at 10-20 ms^{-1}, and atmospheric convection phase translates eastward at 5-10 ms^{-1}). Even the southern hemisphere WWEs, which display an average eastward propagation, translate more lowly at 3-4 ms^{-1}. If there is a connection between MJOs and WWEs it is not clear in the average behavior of WWEs, and must be explored carefully before any generalizations are drawn from a few observed connections. Using the MH98 MJO definition, I also describe statistical relationships between the MJO and WWEs.

I also explore the relationship between WWEs and tropical cyclone activity, which has been made possible by the cataloguing of cyclone tracks. The suggestion that there is a relationship between the cyclones and WWEs dates from the early exploration of westerly wind activity in the central equatorial Pacific. Keen (1982) described the relationship between paired cyclones on either side of the equator and extreme periods of surface westerlies. The relationship was examined again by Harrison and Giese (1991) and the conclusion was that for near-dateline WWEs the relationship is not as strong as originally suggested: ~60% of near-dateline WWEs were associated with tropical cyclone activity. The relationship between cyclones and certain WWEs is suggested by the analysis of surface wind structures of WWEs (Hartten 1996, HV97, Chapter II), where certain WWE types exhibited cyclonic circulation patterns and translation consistent with the main cyclone tracks in the respective hemispheres (towards the northwest in the northern hemisphere, towards the east-south-east in the southern hemisphere). This suggested relationship is reemphasized by the OLR analysis shown in Section 3 of this chapter: the westernmost WWE types (NW and W) displayed tight convective signals which propagate northwestward, and the southern hemisphere WWEs displayed some convective structures which translate eastward.

In the remainder of this chapter I will summarize the work into cataloguing the general relationships between WWEs and tropical convection. Section 2 will describe the

data and methods used. The results of compositing OLR anomaly and surface wind anomaly for each WWE type and for the MJO are described in Section 3. Section 4 summarizes the inter-WWE time spacing results, which indicate that the 40-80 day spacing one would expect from an MJO driven phenomenon is not prominent in most WWE types. Section 5 summarizes the co-occurrence between WWEs and the MJO. Section 6 examines relationships between WWEs and tropical cyclones. Finally, Section 7 gives summarizes and discusses the results.

IV.2. Data and Methods.

The European Centre for Medium Range Weather Forecasts (ECMWF) 12-hourly 2.5°∞2.5° gridded 10-meter wind operational analysis (European Centre for Medium Range Weather Forecasts 1989), and the method described by HV97 and Chapter II were used to identify all the WWEs in the period 1986-1998 (see Table IV.1 for a summary of the identified WWEs). Daily NOAA Interpolated Outgoing Longwave Radiation (OLR), on a 2.5°∞2.5° global grid from 1986-1998 was provided by the NOAA-CIRES Climate Diagnostics Center, Bolder, Colorado (available from their web site: *http://www.cdc.noaa.gov*). The SST used in this analysis is the Reynolds/NCEP weekly 1°∞1° gridded SST product (Reynolds and Smith 1994).

Monthly climatologies of SST and OLR were generated using the weekly SST and daily OLR, respectively, data from 1984 through 1996 (those years are chosen to exclude the very anomalous periods of 1982-3 and 1997-8). Monthly climatology of 10-m wind (**U**) was generated using the 12-hourly data from ECMWF for the period 1986-1995 (for consistency with HV97). SST anomaly (SSTA), OLR anomaly (OLRA) and 10-m wind anomaly (**UA**) were computed from the corresponding monthly climatology. The analysis was repeated using other climatologies, and none of the principal results were affected.

For reference, the climatological convection and SST fields for the months of March,

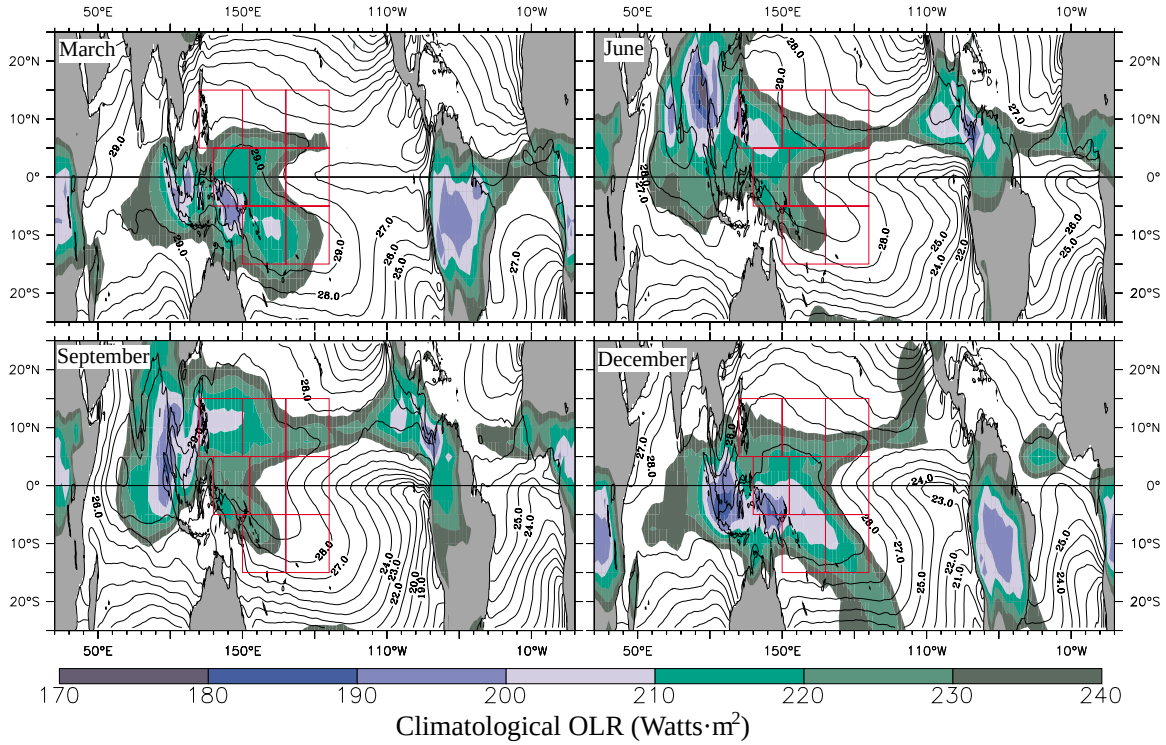

Figure IV.1: Climatological OLR (shading) and SST (contours). Units are °C for SST and Watts·m^{-2}. Contour interval for SST is 1°C, shading interval for OLR is 10 Watts·m^{-2}.

June, September and December are shown Figure IV.1; contoured is SST at 1°C intervals and shaded is OLR values less than 230 Wm^{-2}. Notice the seasonal meridional migration of the warm pool (waters warmer than 28°C) and western Pacific convection fields. Also evident is the seasonal cycle of the eastern Pacific cold tongue in SST, and the Pacific Intertropical and south Pacific convergence zones.

In Chapter III, Section 2, and VH00 the NIÑO3 SSTA distribution was examined over the period 1986-1998, and it was determined that an adequate description of the distribution is of having three states: COOL (NIÑO3 < -0.75°C), REGULAR (|NIÑO3| - 0.75°C) and WARM (NIÑO3 > 0.75°C). Table IV.1 summarizes the number of WWEs of each type identified during the period 1986-1998, and breaks down their distribution based on the NIÑO3 SSTA (SSTA averaged over 150°W-90°W, 5°S-5°N) 20 days prior to the WWE center day.

The bootstrap compositing technique used in Chapter III and VH00 to explore the

SSTA evolution associated with WWEs was applied to the OLR and 10-meter wind data. Because of the large OLRA and **UA** associated with the ENSO phenomenon, the compositing of OLRA and **UA** is performed separately for periods of initially near normal and warmer than normal NIÑO3 SSTA (Cases REGULAR and WARM). The compositing analysis is not performed for periods of initially cooler than normal NIÑO3 SSTA (case COOL), since there are not enough WWEs in that state to perform reliable statistics (see Table IV.1). For the period 1986-1998 ,composites of OLRA are generated for each WWE type, and for each initial NIÑO3 state; the composites go from event Day(-20) to Day(20). As in Chapter III and VH00, I also generated NON-WWE composites, by bootstrap sampling all those dates which are more than 10 days from a given WWE-type center day. Each WWE composite is compared to the corresponding NON-WWE composite, to determine the composite OLRA or **UA** deviation (OLRD, **UD**) from the expected mean. Statistical significance, against a mean of zero, is determined for all composited quantities using a bootstrap method.

A quantitative definition of MJO events was developed by MH98 using the first two empirical orthogonal functions (EOFs) of 30-100 day bandpassed 850 HPa zonal wind. The

Table IV.1: Number of WWEs and MJOs identified in the period Jan. 1986- May 1998. The number of events for each type are listed, along with the breakdown based on NIÑO3 SSTA state 20 days before the WWE center day (or on Phase 4 for the MJOs). The final row lists the percentage of total time in each NIÑO3 SSTA case.

WWE Type	**All Time**	**Case Warm** (NIÑ03>0.75ºC)	**Case Regular** (|NIÑ03|-0.75ºC)	**Case Cool** (NIÑ03 < -0.75ºC)
NW	72	24%	68%	8%
N	37	32%	62%	5.4%
NE	44	39%	50%	9%
W	41	27%	73%	
C	72	42%	58%	
E	51	62%	37%	
S	51	35%	55%	10%
SE	61	44%	48%	8%
MJO	70	29%	63%	8.6%
Percentage of Time in each NIÑO3 State		28%	61%	11%

global MJO definition and index derived by MH98, using the first two empirical orthogonal functions (EOFs) of the intraseasonal filtered 850-mb zonal wind from the NCEP/NCAR reanalysis wind product (Kalnay et al. 1996). The first EOF (which explains 32% of the variance) has a maximum over the central Indian Ocean; the second EOF (which explains 23% of the variance) has a maximum over the Maritime Continent and the western Pacific Ocean. Their principal component timeseries (PCs) are in quadrature,and together they describe and eastward propagating oscillation of 850-mb zonal winds. The MH98 MJO index is generated by adding the first PC with the backward time-shifted second PC; the index has maximum (minimum) values when Indian Ocean 850-mb westerlies (easterlies) are followined by western Pacific westerlies (easterlies). MJO events are defined by identifying times when the local maximum in the index exceeds one standard deviation and is surrounded by local minima with negative index values. The maximum is labeled Phase 5 and the leading (trailing) minimum is labeled Phase 1 (9); Phases 3 and 7 are at the intervening zero crossings of the index, and the "even" Phases (2,4,6,8) are at the midpoints between the surrounding "odd" Phases. Using the different dates identified for each Phase, composites for various quantities can be generated by averaging (as in MH98). The average length of each Phase is close to five days. See Table IV.1 for a breakdown of the number of MJO events identified. Notice that the distribution of MJO events within the three NIÑO3 SSTA states is not significantly different from a uniform distribution (even at the 85% confidence level).

Defining as an index of MJO-activity the 240-day running count of MJO events, a timeseries of MJO-activity can be generated using the MH98 MJO index (henceforth MH-MJOI) from January 1979 through March 1998. The MJO-activity index is plotted along with the NIÑO3 SSTA index in Figure IV.2 (Note that the results are unaffected if the MJO-activity index is computed using anything from the 380 day to 150 day running count). There is a lack of connection between the two indices, which is evident in the correlation

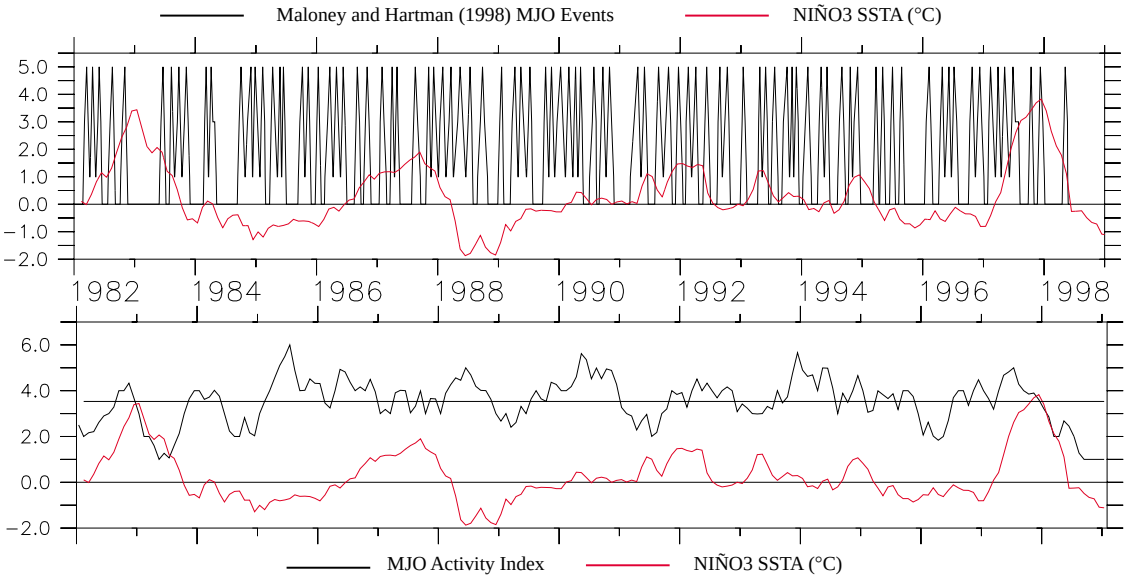

Figure IV.2: Upper panel shows the time-series of MJO events and of NIÑO3 SSTA for the period Jan. 1982-Mar. 1998. Lower panel shows the time-series of MJO activity and of NIÑO3 SSTA for the same period. MJO activity is defined as the 240-day running count of MJO events. Notice the lack of connection between the MJO-activity index and NIÑO3 SSTA.

coefficient of -0.16 at zero lag, which is not significant even at the 85% confidence level. Figure IV.3 shows the 1982-1998 lagged correlation between NIÑO3 SSTA and the MJO Activity Index, with the dashed lines indicating the 90% confidence interval (assuming 24 degrees of freedom and computed as in Appendix A), notice how the only statistically significant correlation (and marginally so) between the quantities is approximately -0.4 at -18 months lag, with increased NIÑO3 SSTA leading reduced MJO activity.

Examining only extreme periods of MJO activity in Figure IV.2, three of the primary maxima of the activity index occur during cold or normal years (cold 1985 and 1988, near-normal 1990), one during a mildly warm year (1994), and one maximum occurs in early 1997 (coincident with the development of the 1997-8 El Niño); the largest minimum occurs during the warm event of 1982. These results are consistent with recent analyses of other MJO indices, which found no significant relationship between increased MJO activity and common El Niño indices (Slingo *et al.* 1999, Hendon *et al.* 2000, Harrison and Vecchi 2000). This should be contrasted with the significant correlations between Troup-SOI and certain WWEs (see HV97 and Chapter II), and with the NIÑO3 SSTA warming

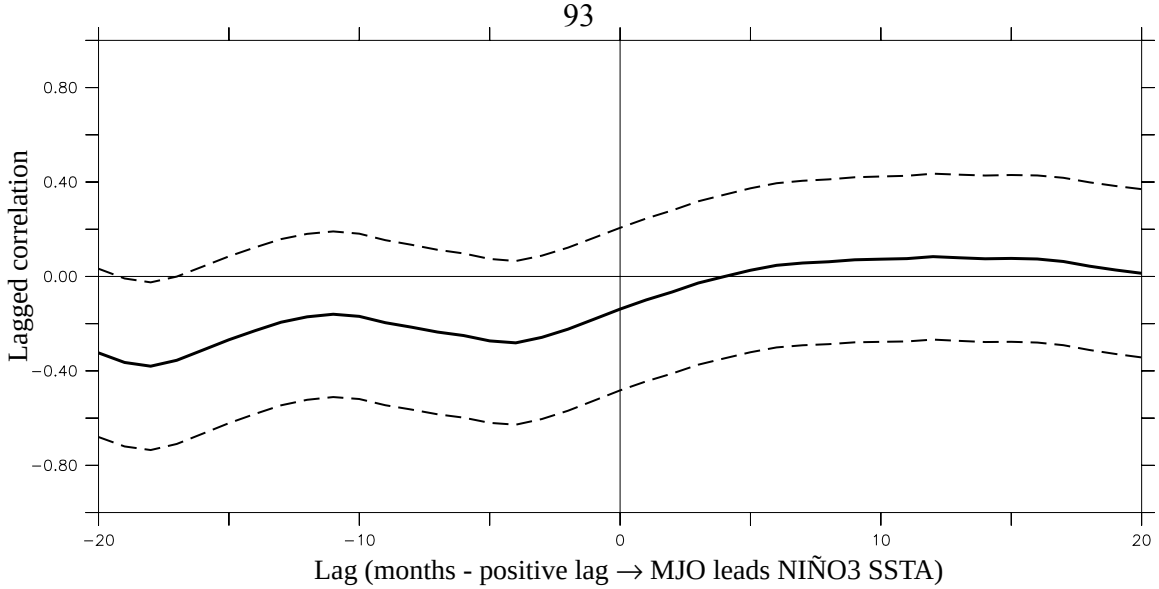

Figure IV.3: Lagged correlation between MJO activity index and NIÑO3 SSTA index. Lag is in months, with positive lag indicating the MJO activity leads NIÑO3 SSTA). Dasshed lines indicate the 90% confidence interval on the correlation.

which tends to follow equatorial WWEs (see VH00 and Chapter III).

Using the MH-MJOI from January 1986 through May 1998 I generated composites of the MJO related atmospheric convection and surface wind fields, for each MJO phase and for both initially WARM and REGULAR conditions. These composites represent the average surface expression of the MJO, and are compared to the WWE OLRA and **U**A composites (see Section 3). I also explore statistical relationships between the various WWE types and MJO events as defined by the MH-MJOI (see Section IV.5).

Tropical cyclone best track data was used to compare tropical cyclone activity to WWE activity, over the period 1986-1998. Eastern tropical Pacific northern hemisphere data was compiled by Dr. Christopher Landsea at Colorado State University (available on-line at: *http://weather.unisys.com/hurricane/)*. Southern hemisphere and western Pacific northern hemisphere cyclone best track data was compiled by the U.S. NAVPACMETOC Center and the Joint Typhoon Warning Center, and can be found on the web at: *http:// www.npmoc.navy.mil/products/jtwc/best_tracks/.* These hurricane data are used to examine relationships between WWEs and Pacific Ocean tropical cyclones over the period 1986-1998. Intensity groupings of the cyclones was done based on the Saffir-Simpson Scale. The

(a) Northwest Pacific cyclone tracks (1987)

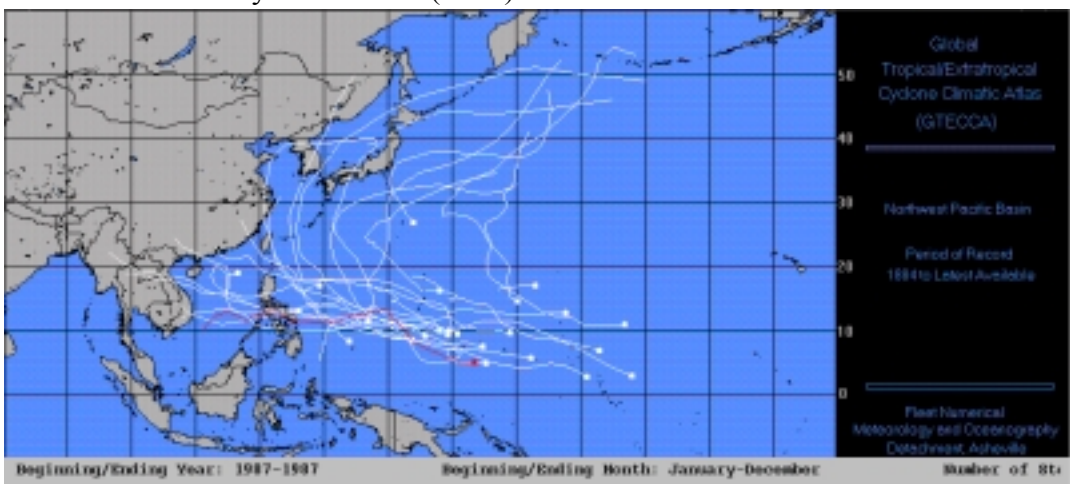

(b) Southwest Pacific cyclone tracks (1987)

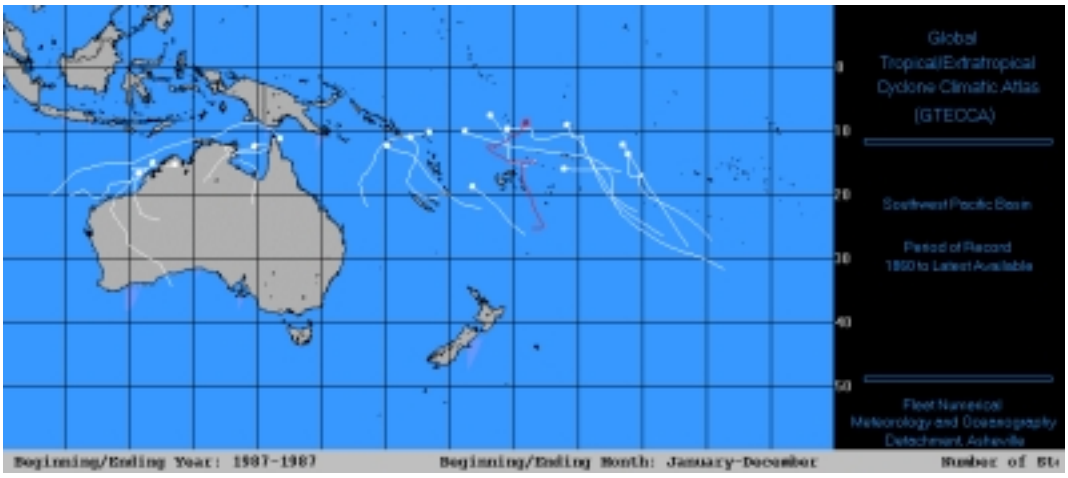

Figure IV.4: Tropical cyclone tracks in the western Pacific in 1987. (a) Tracks for north-west Pacific cyclones, (b) for south-west Pacific cyclones. Data from the Global Tropical and Extra-Tropical Cyclone Atlas (GTECCA 1998).

classifications used here are: a *Tropical Cyclone* is any tropical cyclone catalogued in the atlases regardless of intensity, a *Hurricane* is a tropical storm whose maximum hourly averaged surface winds exceed 74 knots at any point, and a *Category 2 Hurricane* is a Hurricane whose maximum hourly averaged surface winds exceed 96 knots. Tropical cyclone tracks from the Global Tropical and Extratropical Cyclone Atlas (GTECCA 1998) in 1987 are plotted in Figure IV.4. Notice how northern hemisphere western Pacific cyclones tend to translate west-north-westward, while southern hemisphere cyclones tend to translate south-eastward.

WWE Type	Northern Hemisphere Cyclones	Southern Hemisphere Cyclones
NW	130ºE-155ºE; 12ºN-25ºN	
N	150ºE-180ºE; 12ºN-25ºN	
NE	170ºW-140ºW; 20ºN-30ºN	
W	135ºE-160ºE; 0º-15ºN	145ºE-160ºE; 15ºS-0º
C	150ºE-175ºE; 0º-15ºN	150ºE-175ºW; 15ºS-0º
E	180º-150ºW; 0º-15ºN	180º-150ºW; 15ºS-0º
S		150ºE-170ºW; 20ºS-10ºS
SE		170ºE-140ºW; 25ºS-12ºS

Table IV.2: List of regions used to compare tropical cyclone activity to WWE activity. These are referred to as "regions of interest" in the text. They are the places where one might expect a relationship to exist between WWEs and tropical cyclones.

To explore the relationship between cyclones and WWEs methodically, cyclone regions of interest for each WWE are defined. These regions of interest are where cyclone activity might be expected to be related to WWE activity, based on the surface wind analysis, the OLR composites and the structure of tropical cyclones (which have westerly circulation equatorward of the eye). The regions of interest for each WWE type are listed in Table IV.2. For off-equatorial WWE types, only cyclones in the corresponding hemisphere are examined; for equatorial WWEs, cyclones on either side of the equator are examined.

In order to be able to discuss the various degrees of statistical association that WWEs have to cyclones and to the MJO, the term "characteristic" will be used to denote a particular statistical relationship. A property X is defined to be *characteristic* of a phenomenon Y if the conditional probability of X being true given Y has occurred is much greater than the conditional probability of X being false given Y has occurred (X is defined as a characteristic of Y if $P(X|Y) >> P(\sim X|Y)$). Since I will be dealing with simple systems where X and Y are exclusively true or false, $P(\sim X|Y) = 1-P(X|Y)$. The definition of characteristic can be simplified to having $P(X|Y) > t$, where t is some threshold. For the remainder of this discussion, t is chosen to be 85%. Note that characteristic as defined here is independent of statistical significance, rather it refers to whether a particular feature is likely to be found associated with a phenomenon. A feature might be significant and not characteristic, or vice-versa.

IV.3. OLR Composite results.

This section summarizes the results of compositing OLRA and **UA** for the MJO and for each WWE type. Tropical Pacific atmospheric convection and surface wind have large interannual variability associated with ENSO, which should be removed to observe only the WWE or MJO related convective and wind signals. When examining the composite OLR variability associated with each WWE type or the MJO separately for WARM and REGULAR cases we will focus of the OLRA and **UA** departure from the expected mean in the absence of the particular WWE type or MJO Phase (the quantity defined as OLRD and **UD** in Section 2).

a. MJO Composites:

First I examine the evolution of the MJO related OLRA and **UA** fields for all MJO events, regardless of NIÑO3 SSTA. The **UA** results are analogous to the WWE wind anomaly composites described in Chapter II and HV97. Figure IV.5 shows the 99% significant OLRA and **UA** all time MJO composite; shaded are values of OLRA significant at the 99% level, vectors indicate **UA** when either vector component is significant at the 99% confidence level (significance determined using a bootstrap method). The expected anomalies when all time is considered, are close to zero, so OLRD and **UD** are very similar to OLRA and **UA** in the all event composite (Figure IV.5). Each Phase of the MJO is as defined in Maloney and Hartmann (1998); the average duration of a Phase is five days.

Phase 1 of the MJO is associated with reduced convection north and south of the equator over the eastern Indian Ocean; there are easterly anomalies west of the convection anomalies. There is also enhanced convection north of the Equator over Central America and northern South America, with weak westerly anomalies generally in the Pacific ITCZ region. During Phase 2 there are no large-scale convection anomalies, but there are large regions of easterly (westerly) in the off-equatorial tropical Indian Ocean (eastern tropical north Pacific). In Phase 3, enhanced convection exists over the western equatorial Indian

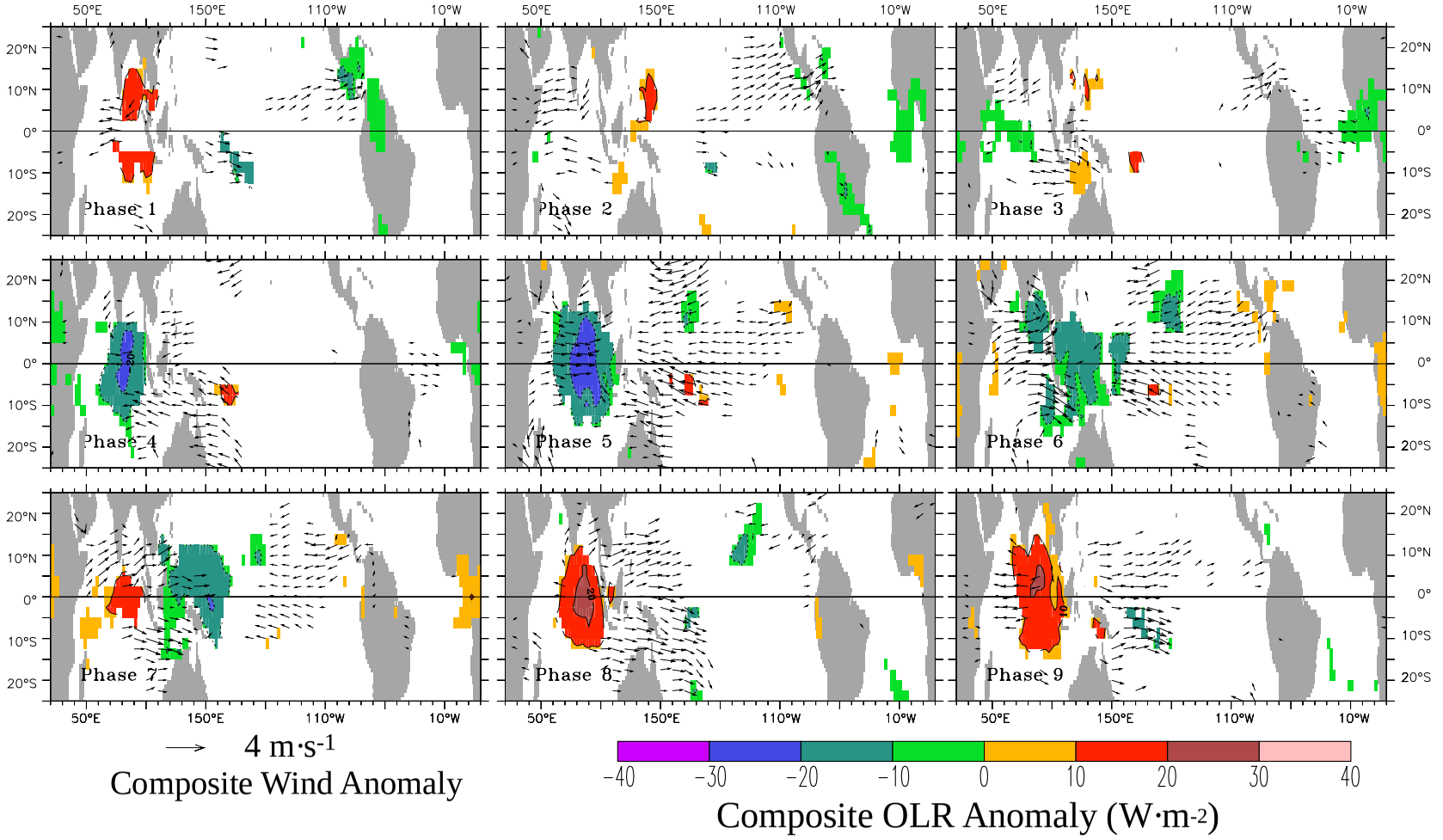

Figure IV.5: All-event composite MJO OLRD and **UD** for each of the nine MJO Phases. Cool (warm) colors indicate enhanced (reduced) convection. OLRD is shaded if significant at the 99% confidence level. UD vectors are drawn if either the zonal or meridional component is significant at the 99% confidence level.

ocean with easterly anomalies north of it and southeast of it. There are southeasterly anomalies from the Pacific ITCZ across Central American into the southern Caribbean, with no associated convective anomalies.

Phase 4 exhibits enhanced convection over a large part of the eastern Indian Ocean, and easterly anomalies across much of the western Pacific and southeastern Indian Oceans. During Phase 5 (the Phase with maximum central Indian Ocean 850 hPa westerlies – MH98) the Indian Ocean enhanced convection has grown in size and intensity, but its center has not moved much; now there are westerly anomalies west of and within the convection region, and easterly anomalies broadly across the central and western tropical Pacific. Phase 6 has the region of enhanced convection over the Maritime Continent, with westerly anomalies covering much of the tropical Indian Ocean, and easterly anomalies covering much of the eastern and central tropical Pacific. During Phase 7 there is a convective anomaly couplet, with enhanced convection still over the Maritime Continent and reduced convection in the central and eastern equatorial Indian Ocean. Westerly anomalies continue north and south of the region of reduced convection and, weakly, into the region of enhanced convection. Easterly anomalies exist broadly in the central tropical Pacific between 10°N and 10°S. Only during Phases 8 and 9 are the dominant Pacific wind anomalies westerly. In Phases 8 and 9, there is weakly enhanced convection over the central Pacific, and strongly reduced convection over the central and eastern Indian Ocean. There are westerly anomalies generally over the western Pacific between 15°N and 15°S and the flow is generally divergent at the surface, with a northerly (southerly) component north (south) of the equator and with only a small area of equatorial westerly anomalies.

The periods of enhanced convection over the western Pacific are Phases 6 through 8, and there are corresponding periods of reduced convection in Phases 2 through 4. This OLRA field is qualitatively consistent with the MJO OLRA evolution described in the literature (Rui and Wang 1991, Madden and Julian 1994). The convective anomalies propa-

gate at an average speed of 5-10 ms^{-1} (depending on whether the Phase length is between 5 and 10 days).

A feature to notice, and contrast with the OLR evolution and recent models of the MJO surface wind field, is the asymmetry of the surface zonal wind circulation over the tropical Pacific. A prominent surface wind feature are the easterlies across most of the western and central Pacific during MJO Phases 4 through 7. There is no corresponding Phase of strong westerlies across the basin, rather the westerlies tend to be confined to an area west of the dateline. The amplitude of the wind anomalies over the central equatorial Pacific is roughly half that over the western Pacific, but the easterly anomalies tend to occur in a region of strong easterly trade winds, while the westerlies occur over a region of weak climatological winds (see Figure II.3). Since wind stress is proportional to the square of the wind speed, the momentum flux due to the central/eastern Pacific anomalies could be comparable to that associated with the western Pacific anomalies. Notice also how the largest amplitude wind anomalies tend to be far off equator (>5°), beyond the oceanic equatorial waveguide.

Since the interactions which couple the tropospheric MJO circulation with the atmospheric boundary layer circulation are generally a function of the background atmospheric circulation and of SST, I now examine the MJO related surface circulation for periods of near normal NIÑO3 SSTA separately from periods of warm NIÑO3 SSTA. As with the compositing of SSTA following WWEs in Chapter III, one would ideally like to perform the compositing for different seasons as well as for different NIÑO3 SSTA states; however, since there are only 13 years of wind data available, the analysis is performed only for different NIÑO3 SSTA states. This analysis will examine the statistically significant OLRA and **UA** deviations from the expected anomalies (defined as OLRD and **UD** in Section 2), for MJO phases when NIÑO3 SSTA is in the REGULAR state (Figure IV.6) and in the WARM state (Figure IV.7). The deviations shown in Figure IV.6 are masked at the

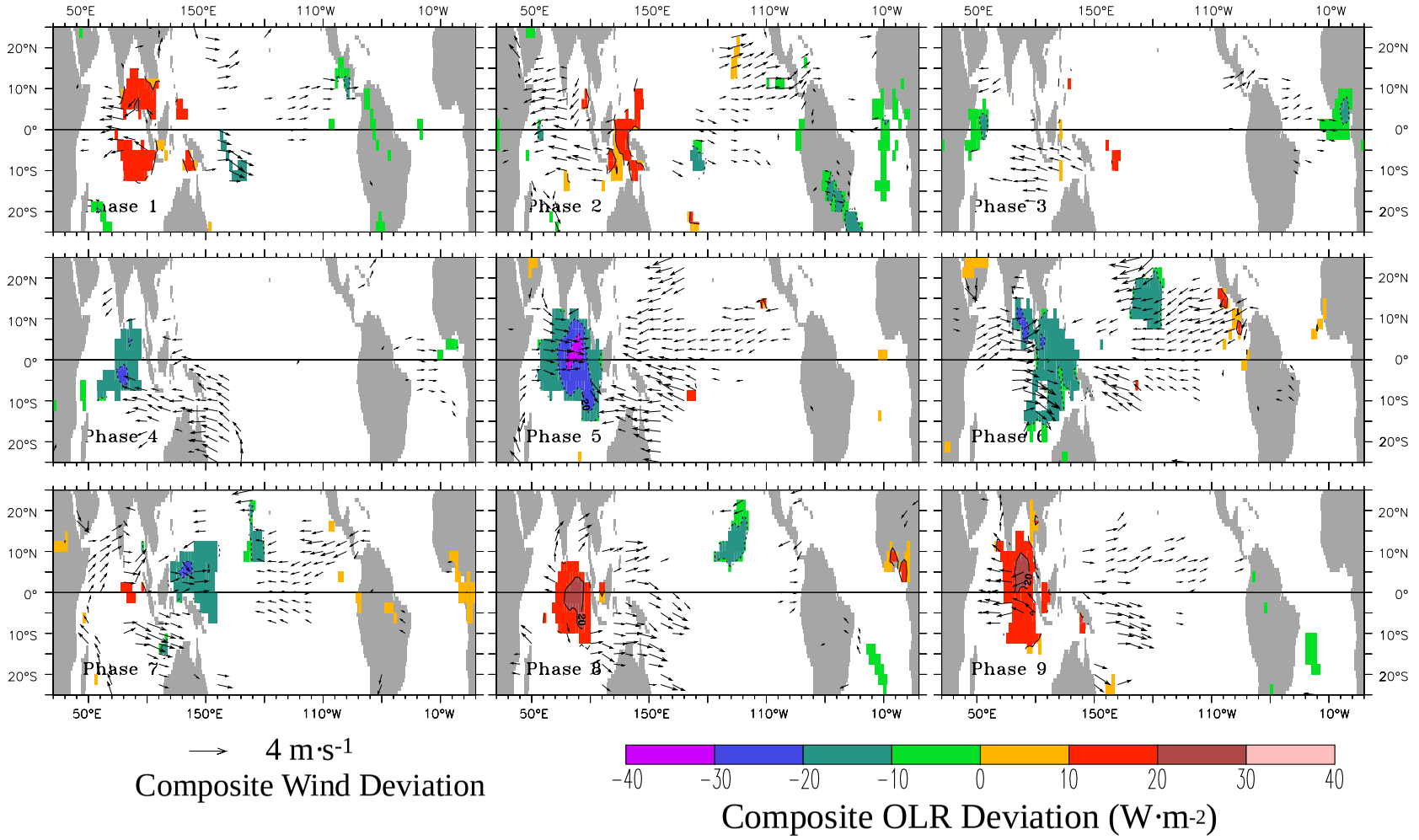

Figure IV.6: REGULAR-event composite MJO OLRD and **UD** for each of the nine MJO Phases. Cool (warm) colors indicate enhanced (reduced) convection. OLRA is shaded if significant at the 99% confidence level. UD vectors are drawn if either the zonal or meridional component is significant at the 99% confidence level.

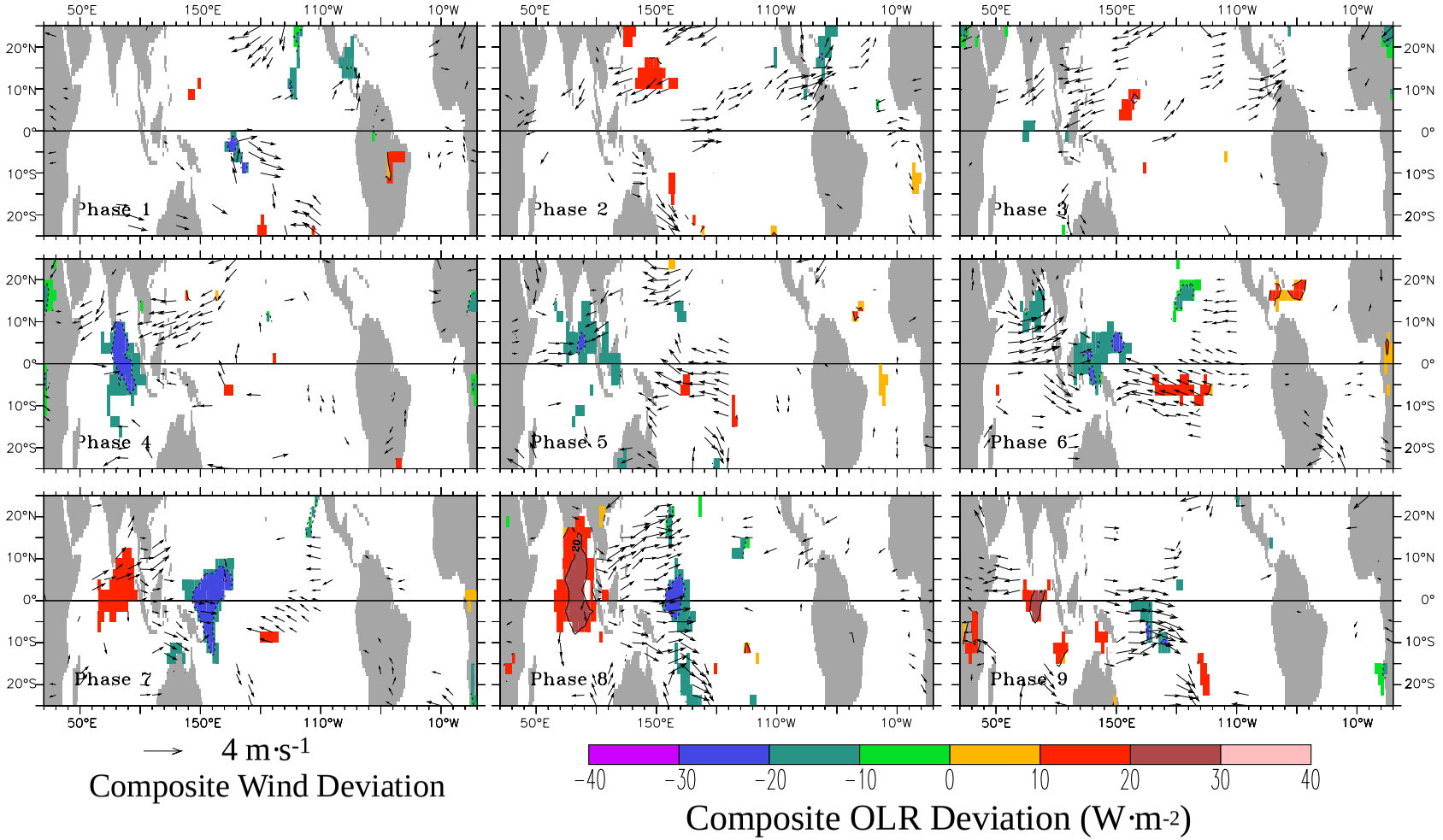

Figure IV.7: WARM-event composite MJO OLRD and **UD** for each of the nine MJO Phases. Cool (warm) colors indicate enhanced (reduced) convection. OLRA is shaded if significant at the 95% confidence level. UD vectors are drawn if either the zonal or meridional component is significant at the 95% confidence level.

99% confidence level; the deviations shown in Figure IV.7 are masked at the 95% confidence level because of the small number of realizations.

Figure IV.6 shows the evolution of the 99% significant OLRD and **UD** fields for the case REGULAR MJO composite. Notice how the fields are qualitatively similar to the OLRA and **UA** fields for the all MJO composite (Figure IV.5). The wind asymmetry in the tropical Pacific is still evident in this composite. Notice how the period of westerlies in the Pacific is MJO phases 6 through 9. The character of the wind and convective deviations in the Case REGULAR composite is essentially that of the convective and surface wind anomalies in the all-event composite.

Figure IV.7 shows the evolution of the OLRD and **UD** fields for the case WARM MJO composite. The evolution in Figure IV.7 is qualitatively similar to that in Figures IV.5 and IV.4, but the amplitude of the Indian ocean convection is smaller and the peak occurs in Phase 4 rather than Phase 5. Here, again, the MJO phases with westerlies in Pacific are Phases 7 through 9. The main difference between the WARM and REGULAR MJO composite is the more persistent westerlies which extend east past the Dateline. This eastward expansion and persistence of the westerlies is likely due to the eastward migration of the western Pacific warm pool east of the Dateline during El Niño events.

b. WWE Composites:

Figure IV-8 shows the *OLRA* and **UA** fields from the ALL/NON-EVENT composites, for both case REGULAR and WARM. The NON-EVENT composites for each of the individual WWE types do not differ in any appreciable way from the ALL/NON-EVENT composite. Notice that when the NIÑO3 SSTA index is near normal and there are no WWEs (Fig. IV.8.a) the main anomalies are enhancements of the climatological state, with enhanced convection over the Maritime Continent, reduced convection east of the dateline and enhanced easterlies along the equatorial Pacific and westerlies over the Indian Ocean. These patterns are due to the fact that there were more warm ENSO (El Niño) events in the

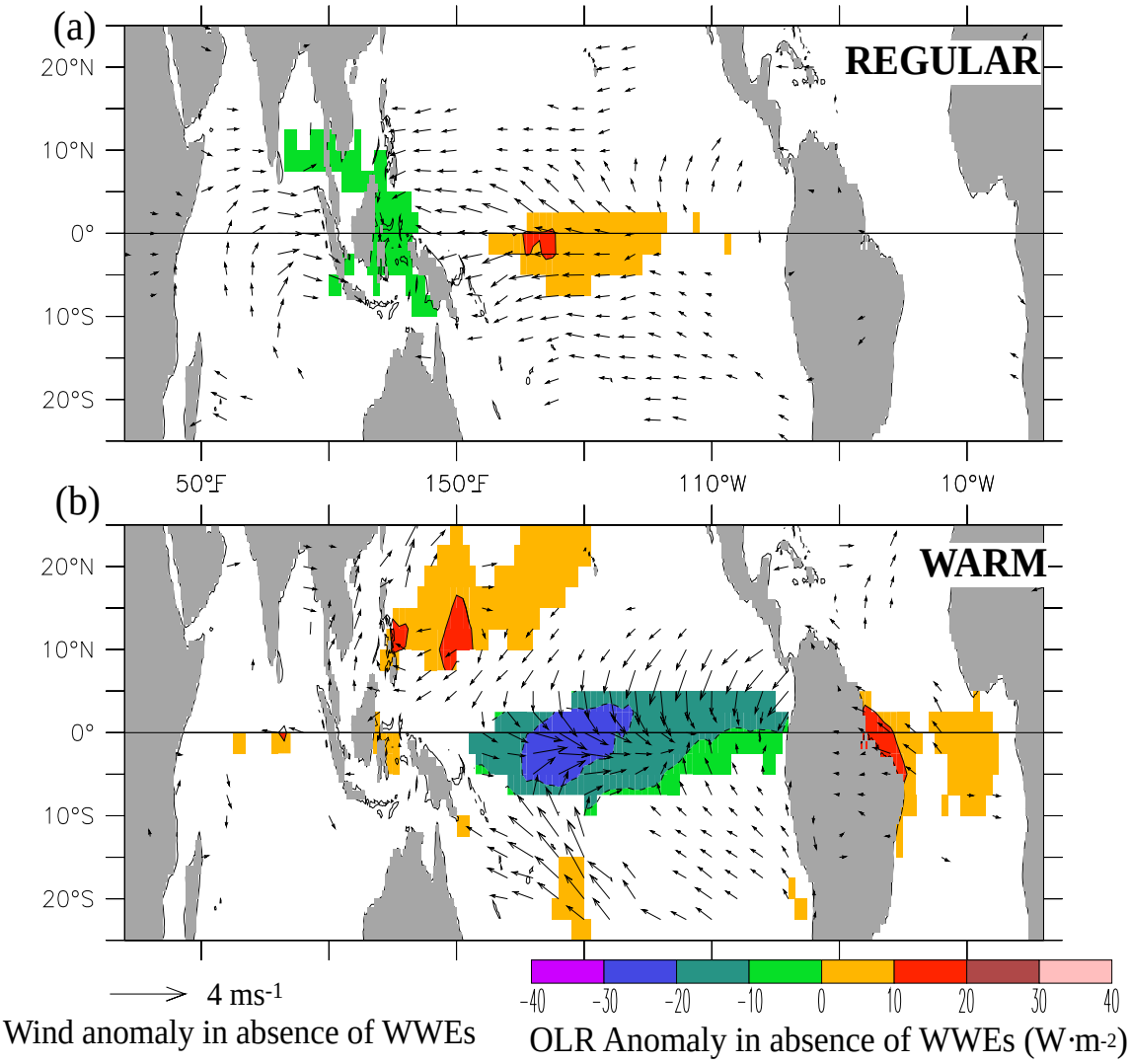

Figure IV.8: 99% significant OLRA and **UA** in the absence of any WWEs (a) when NIÑO3 SSTA is near normal (Case REGULAR), (b) when NIÑO3 SSTA is warmer than noemal (Case WARM).

period 1984-1996 than cold ENSO (La Niña) events, so the climatology is slightly biased towards the warm state of ENSO (When computing OLRD and **UD** the bias is removed). When NIÑO3 SSTA is warmer than normal (Fig. IV.8.b), the convective patterns generally associated with ENSO are evident, as are the surface wind anomaly patterns. The enhanced convection east of the dateline is associated with the eastward migration of the warm pool during ENSO, and the weak equatorial westerlies and meridional inflow to the equator have

been described in previous analyses of the average evolution of ENSO (Rasmusson and Carpenter 1982, Harrison and Larkin 1998). There is also reduced convection over the Amazon basin and the northwestern tropical Pacific when NIÑO3 SST is warmer than normal.

Let us now turn our discussion to the composite OLRD and **UD** evolution associated with the 8 WWE types. Generally, there is reduced OLRA (indicative of enhanced atmospheric convection) in or near the main WWE surface wind anomalies near the WWE center day; there is also enhanced OLRA (indicative of reduced atmospheric convection) over the eastern Indian Ocean and Maritime Continent for many WWE types. The three north-westernmost WWE types (NW, N and W) have propagating convective structures suggestive of a WWE/tropical cyclone connection. The two southern hemisphere (Types S and SE) WWEs have eastward propagating convective structures. The equatorial WWE Type whose main westerly anomalies are just west (Type C) and east (Type E) of the dateline are associated with enhanced convection over the main surface westerlies, with no distinct propagation. The surface wind fields are similar to those described in HV97 and Chapter II.

i) TYPE NW (FIGURE IV.9):

The evolution of the OLRD and **UD** fields in both the WARM and REGULAR case composites is similar. The surface wind evolution in both cases is as described in HV97 and Chapter II, with a cyclonic structure developing and moving towards the northwest. Prior to the formation of the cyclonic structure there are weak westerlies in the classifying region and weakly enhanced equatorial convection. The OLR deviations grow in amplitude and move towards the northwest as the surface winds develop a cyclonic structure and begin to move with the convective anomalies. By Day (6) the convective and surface wind deviations have disappeared. In both cases (REGULAR and WARM) there is some reduced convection in the eastern Indian Ocean near Day (-3). In both cases there are weak equatorial

westerlies on and following the center day near the dateline. The convective and surface wind structures are suggestive of a link between tropical cyclone activity and the Type NW WWE.

ii) TYPE N (FIGURE IV.10):

The case REGULAR and WARM composite OLRD and **UD** fields for the Type N WWE have some qualitative differences, although many general features are the same. The surface wind variability in and near the classifying region is similar in both cases. Both composites have enhanced convection poleward of the main surface westerlies. The case REGULAR composite OLRD does not develop the tight structure seen in the case WARM composite. The case REGULAR composite surface wind deviation has weak equatorial westerlies following the WWE center day, which are not present in the case WARM composite. The case REGULAR composite has weak reduced convection over the Maritime Continent through the lifetime of the WWE. The composite OLRD and **UD** fields are suggestive of a link between Type N WWEs and tropical cyclone activity when the eastern Pacific is warmer than normal.

iii) TYPE NE (FIGURE IV.11):

The convective and wind variability is qualitatively similar in the case REGULAR and WARM Type NE composite WWE. In both cases the main convective structure is a localized region of enhancement, centered near the Hawaiian islands. This convection is evident through the center day, and quickly disappears after it. The wind deviations have a cyclonic structure to them, but the climatological trade winds over the northeast tropical Pacific are so strong that the wind deviations (and anomalies) actually represent near zero winds. The Type NE composite winds are best described as a break in the trade winds.

iv) TYPE W (FIGURE IV.12):

The case REGULAR and WARM composites for the Type W WWE are different in

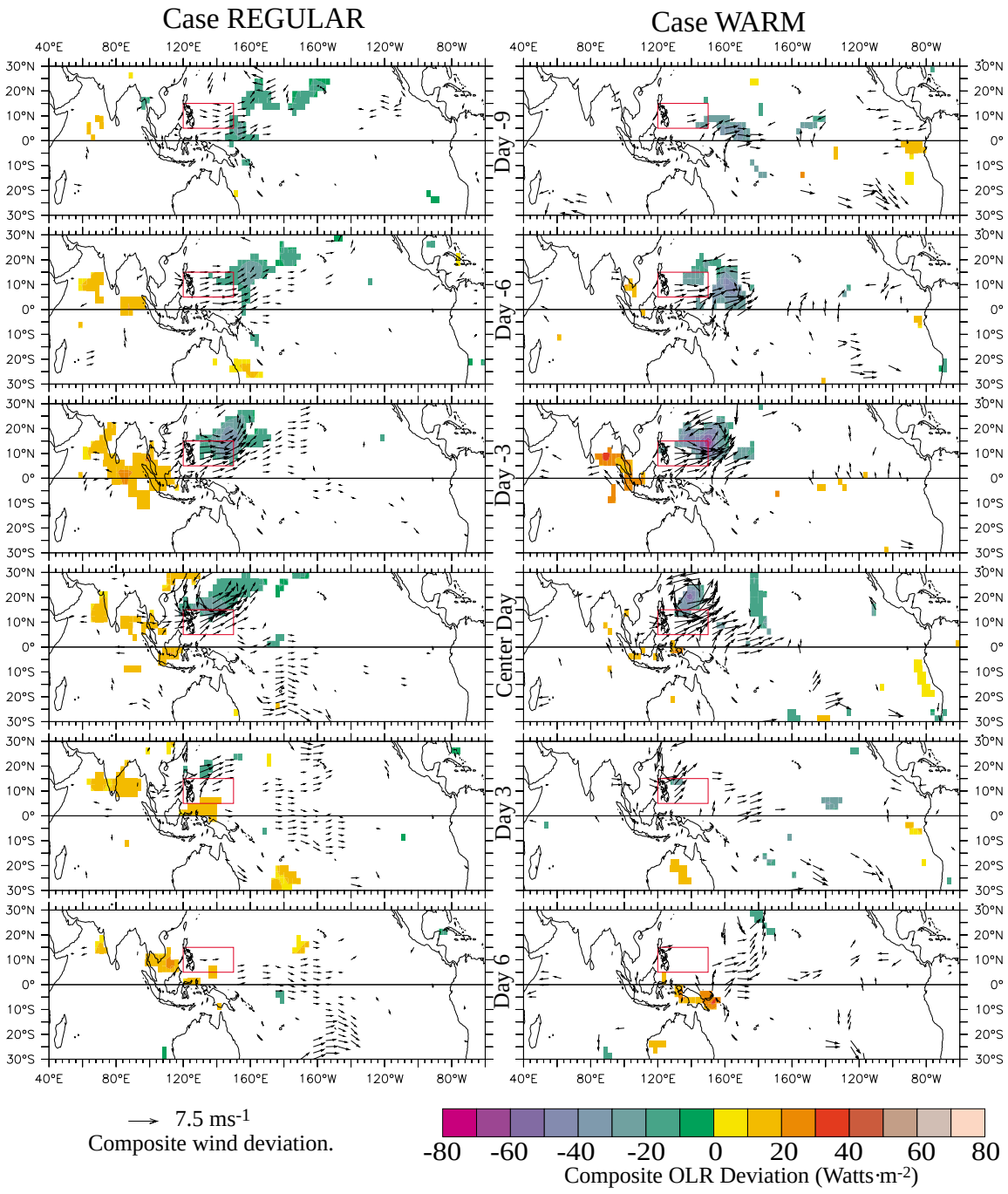

Figure IV.9: Composite evolution of the Type NW OLRD and **UD** fields for (left column) Case REGULAR, (right column) Case WARM. Composite goes from Day (-9) though Day (6) by 3 day intervals. Shaded is OLRD, with cool (warm) colors indicating enhanced (reduced) convection, masked at the 99% confidence level. Wind deviation vectors are plotted if either the zonal or meridional component is significant at the 99% confidence level.

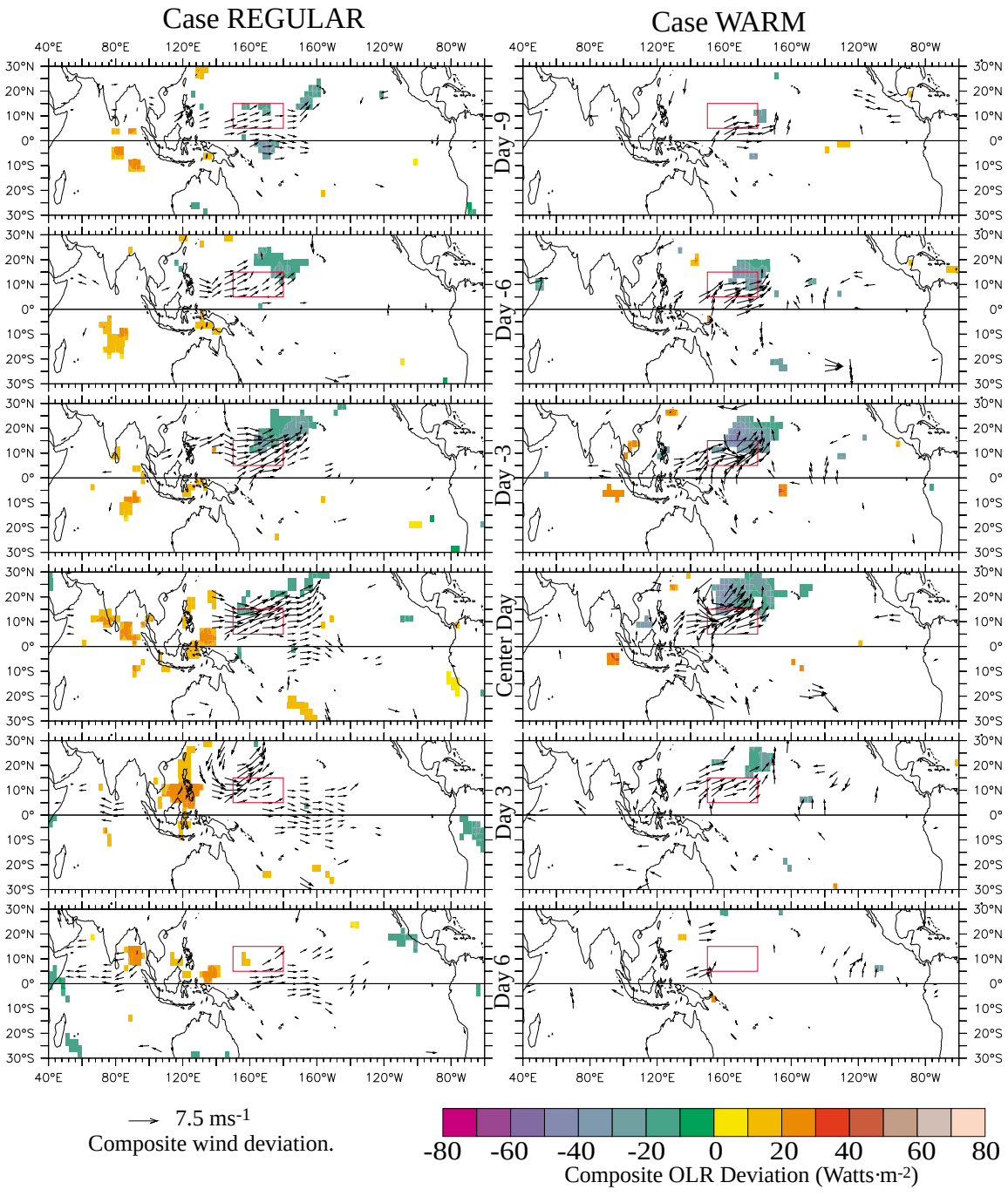

Figure IV.10: Composite evolution of the Type N OLRD and **UD** fields for (left column) Case REGULAR, (right column) Case WARM. Composite goes from Day (-9) though Day (6) by 3 day intervals. Shaded is OLRD, with cool (warm) colors indicating enhanced (reduced) convection, masked at the 99% confidence level. Wind deviation vectors are plotted if either the zonal or meridional component is significant at the 99% confidence level.

many respects, but both composites are indicative of a relationship between Type W WWEs and tropical cyclone activity. The differences between the two composites might be due to the small number of Type W WWEs occurring during when the eastern Pacific SST is warmer than normal; or it might be due to an actual difference in the evolution of the convection and surface wind fields in either case.

In the case REGULAR composite (Fig IV.12.a-.f) there is weak enhanced convection on Day (-9) along with weak equatorial westerlies. The convection and westerlies intensify as the winds develop a cyclonic structure. North of the Equator the cyclonic structure and enhanced convection concentrate and move towards the northwest (note that there is also a concentration of the southern hemisphere convection to the southeast of the classifying region on before the center day). Near the center day there is a reduction of the convection over the Maritime Continent, which continues through Day (6).

The case WARM composite (Fig. IV.12.g-.l) displays more localized regions of significance. On Day(-9) and Day(-6) there is some weak enhanced convection west of the classifying region, with no significant equatorial westerlies. By Day(-3) a strong, tight convectively enhanced feature off the northeastern corner of the classifying region has formed, along with cyclonic winds surrounding it. There is also some weak convection to the southeast of the classifying region. The northern hemisphere cyclonic circulation / convectively enhanced feature propagates to the northwest and dissipates after Day (3). There is an indication of reduced convection over northern Australia following the center day.

v) Type C (Figure IV.13):

The case REGULAR and case WARM **UD** and OLRD composites for the Type C WWE are similar to each other within the WWE classifying region, but there are some striking differences over the Indian Ocean and in the far eastern Pacific off the equator. In the classifying region, the composite for both cases has enhanced convection developing with the equatorial westerlies up to the center day; and disappearing after the center day.

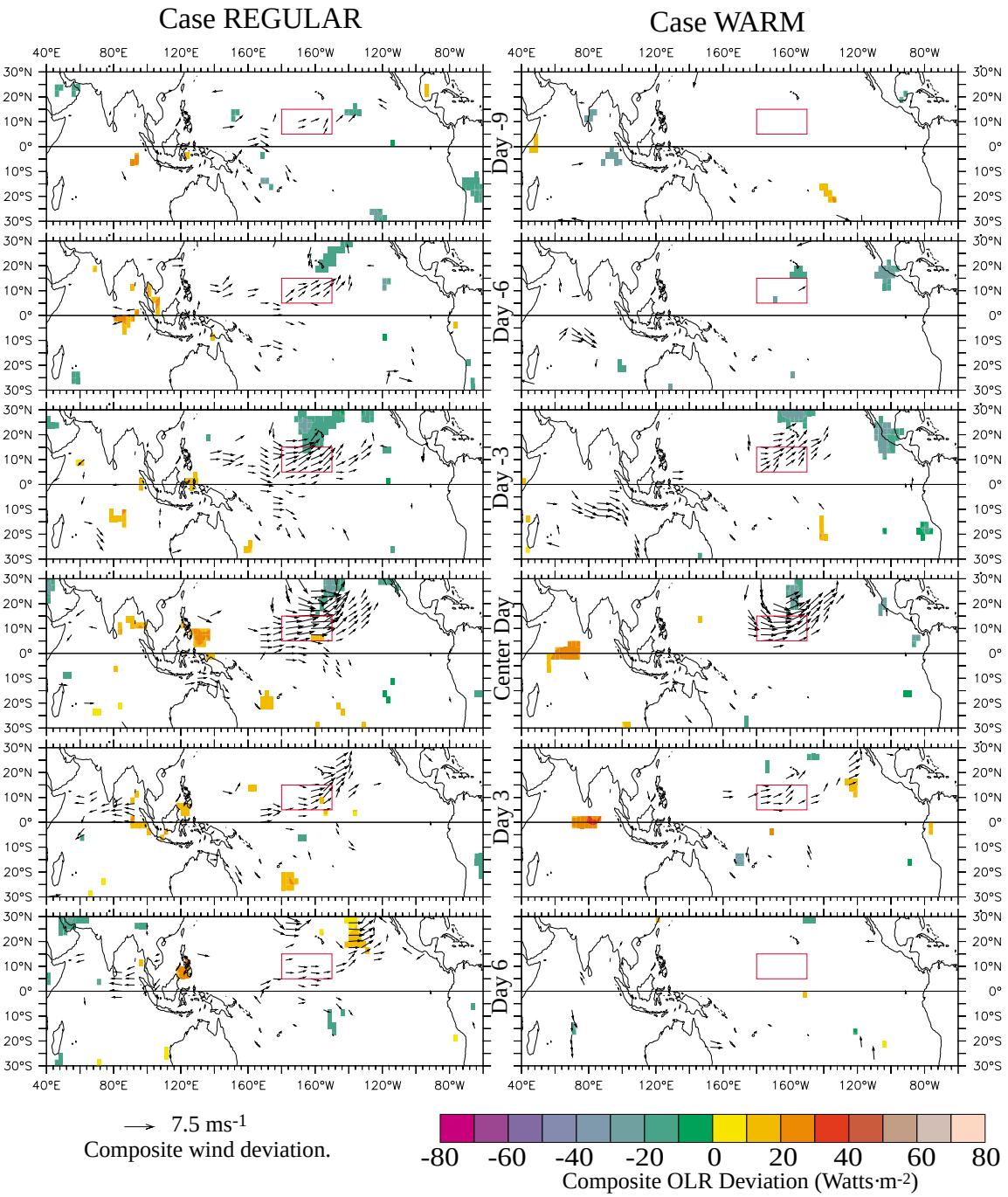

Figure IV.11: Composite evolution of the Type NE OLRD and **UD** fields for (left column) Case REGULAR, (right column) Case WARM. Composite goes from Day (-9) though Day (6) by 3 day intervals. Shaded is OLRD, with cool (warm) colors indicating enhanced (reduced) convection, masked at the 99% confidence level. Wind deviation vectors are plotted if either the zonal or meridional component is significant at the 99% confidence level.

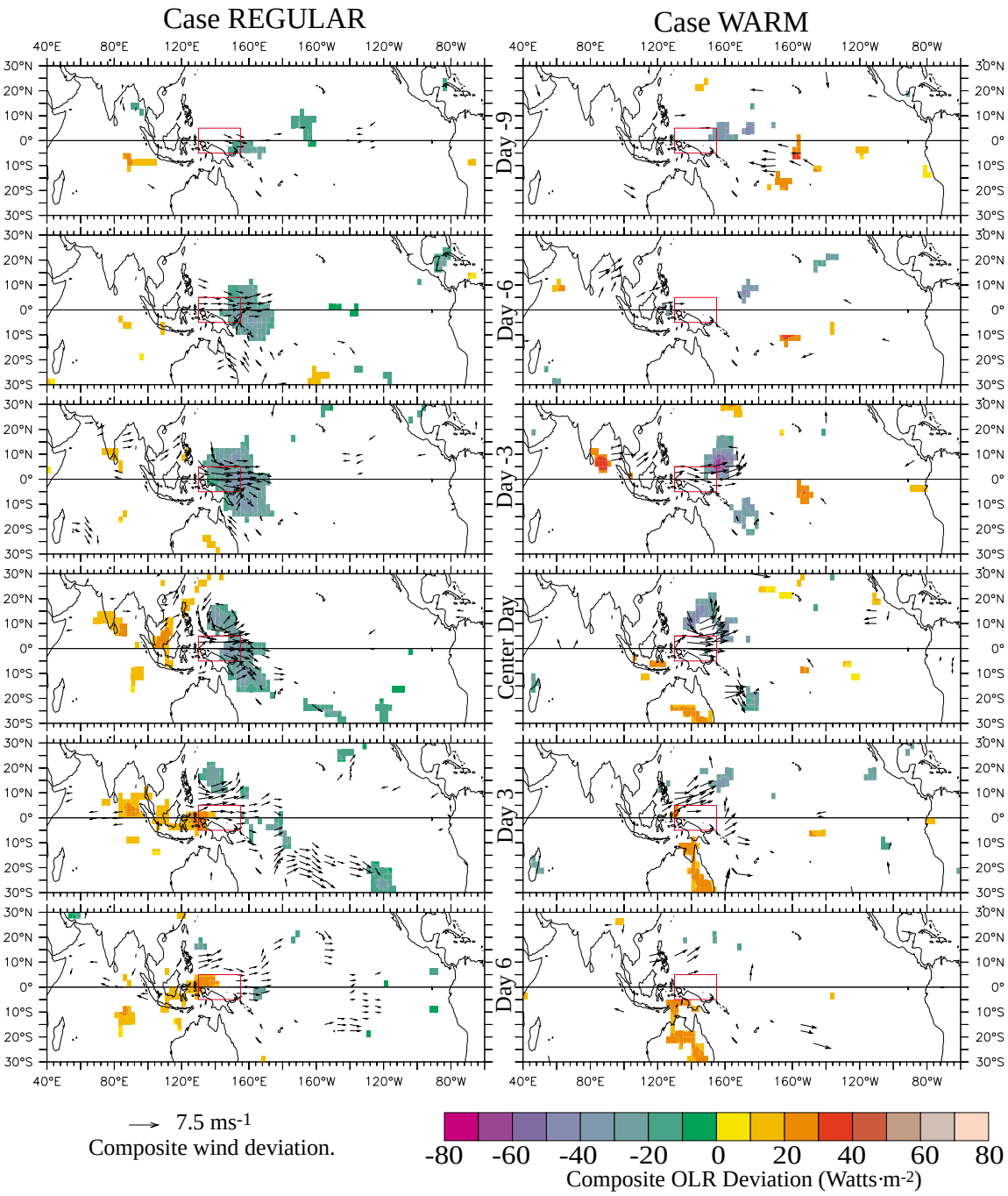

Figure IV.12: Composite evolution of the Type W OLRD and **UD** fields for (left column) Case REGULAR, (right column) Case WARM. Composite goes from Day (-9) though Day (6) by 3 day intervals. Shaded is OLRD, with cool (warm) colors indicating enhanced (reduced) convection, masked at the 99% confidence level. Wind deviation vectors are plotted if either the zonal or meridional component is significant at the 99% confidence level.

The case WARM composite has only scattered wind and OLR deviation patterns far from the classifying region, the main feature is reduced convection over the Maritime Continent beginning near the center day.

Apart from the main WWE anomalies, the case REGULAR composite has reduced convection over the central Indian Ocean beginning on Day (-9) (see Fig. IV.13.a), which appears to propagate east until it reaches the Maritime Continent on Day (-3) (see Fig. IV.11.c), where it remains through Day (9) (not shown). Also evident in the Type C composite is some reduced OLRA over the southeastern Pacific Ocean, centered near 20°S; this feature might not be representative of variability in atmospheric convection since this area is generally covered by marine stratus clouds (Klein and Hartmann 1993). Evident in the case REGULAR **UD** composite are two branches of weak to moderate westerlies centered near 20°S and 20°N, between 160°W and 120°W; these off-equatorial westerlies have no counterpart in the WARM event composite.

vi) TYPE E (FIGURE IV.14):

The case REGULAR and WARM Type E composite OLRD and **UD** fields are similar in and near the classifying region, but there are differences away from the classifying region. The differences between the case REGULAR and WARM OLRD appears to be a matter of amplitude and extent, while the surface wind deviation fields away from the classifying region are qualitatively different.

In the WWE classifying region, significant equatorial westerlies appear by Day (-6) in both cases (see Fig. IV.14.b and IV.14.h), and weakly enhanced convection appears following the westerlies. Reduced convection over the Maritime Continent appears at the same time as the enhanced convection in the classifying region. The reduced convection is of larger extent and amplitude in the case REGULAR composite than in the case WARM composite. In the case REGULAR composite there are moderate westerlies in the northern hemisphere east of the dateline, which appear to propagate eastward beginning on Day (-9)

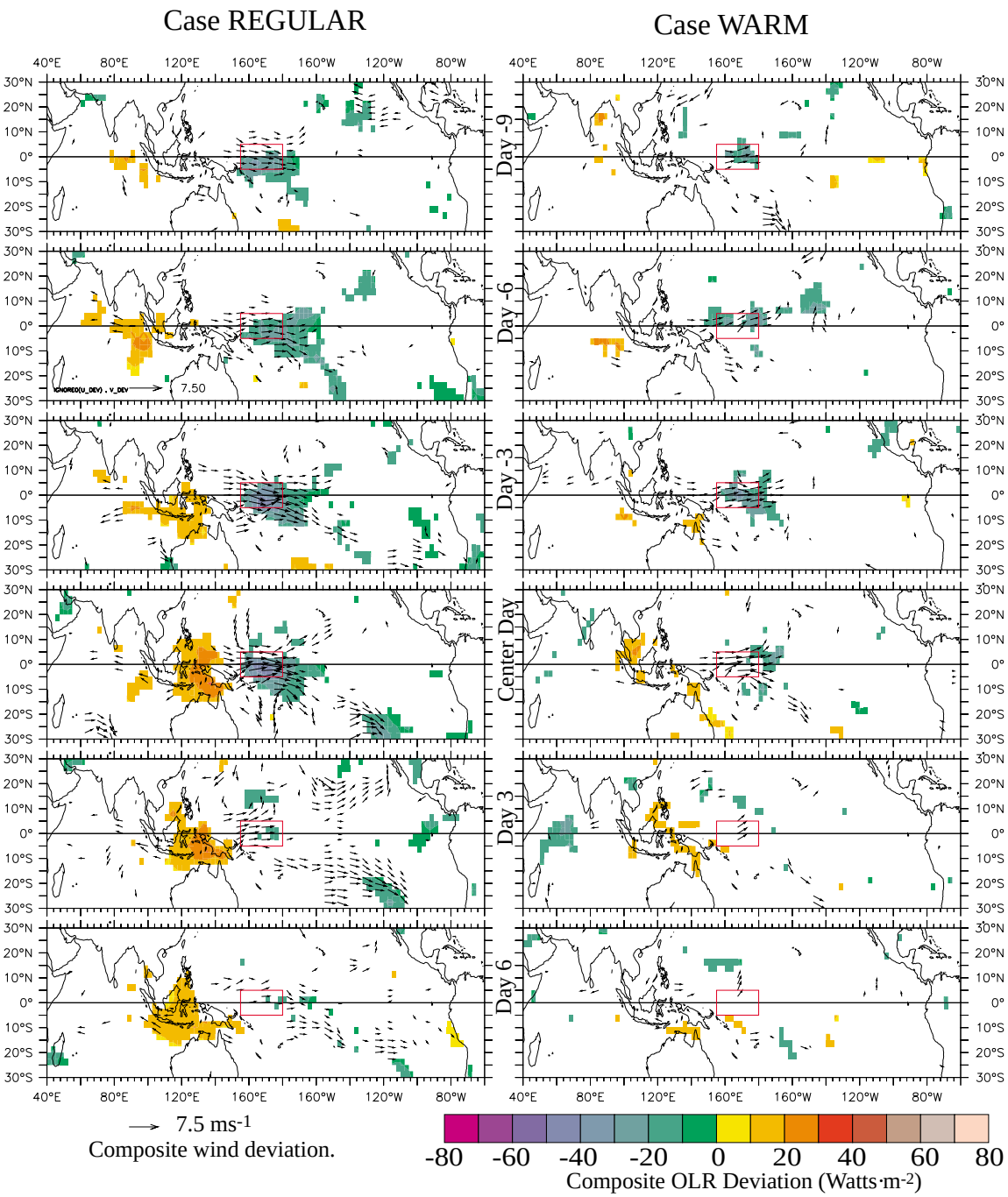

Figure IV.13: Composite evolution of the Type C OLRD and **UD** fields for (left column) Case REGULAR, (right column) Case WARM. Composite goes from Day (-9) though Day (6) by 3 day intervals. Shaded is OLRD, with cool (warm) colors indicating enhanced (reduced) convection, masked at the 99% confidence level. Wind deviation vectors are plotted if either the zonal or meridional component is significant at the 99% confidence level.

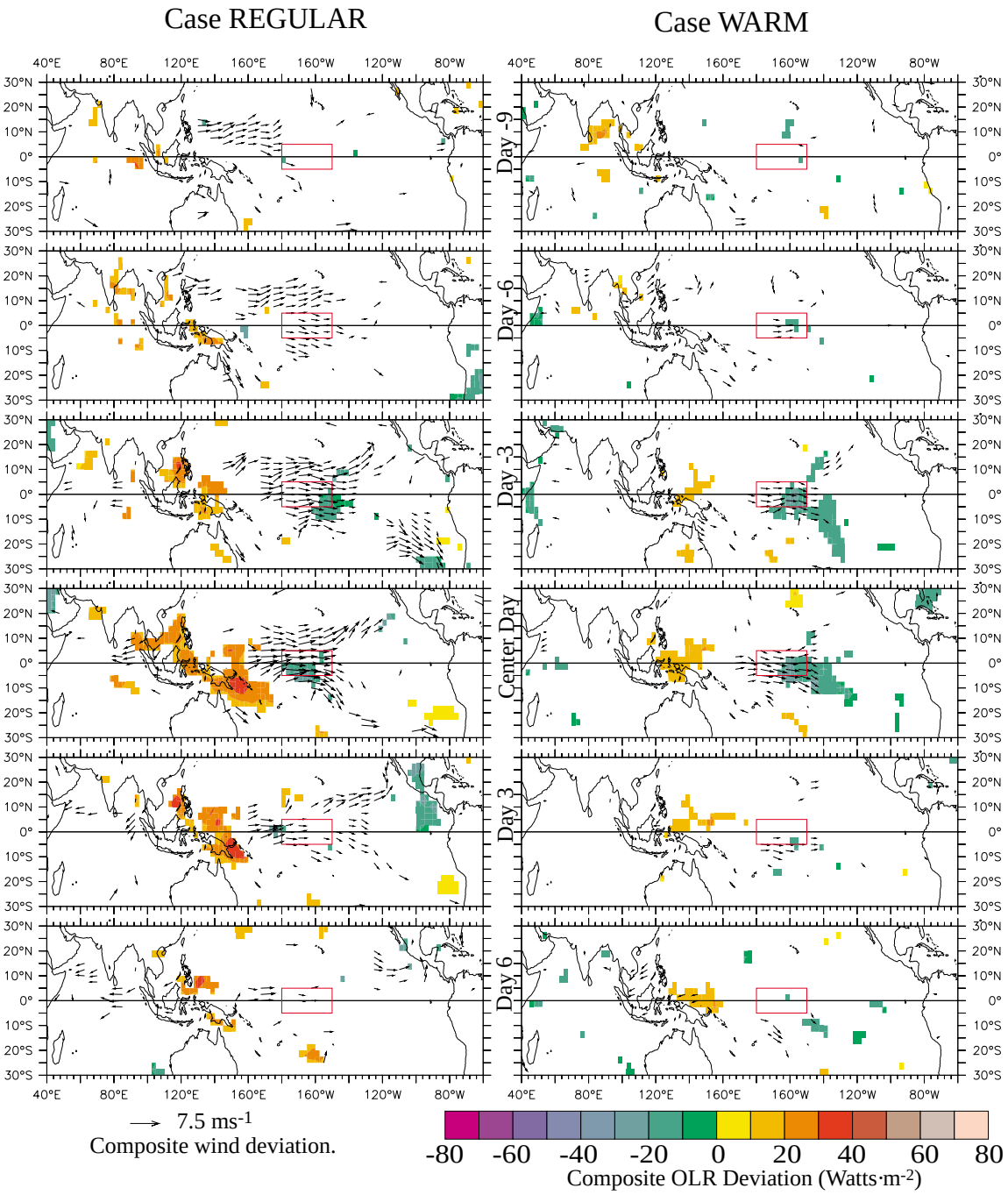

Figure IV.14: Composite evolution of the Type E OLRD and **UD** fields for (left column) Case REGULAR, (right column) Case WARM. Composite goes from Day (-9) though Day (6) by 3 day intervals. Shaded is OLRD, with cool (warm) colors indicating enhanced (reduced) convection, masked at the 99% confidence level. Wind deviation vectors are plotted if either the zonal or meridional component is significant at the 99% confidence level.

and they appear to meld into the equatorial westerlies by the center day.

vii) TYPE S (FIGURE IV.15):

The case REGULAR and WARM Type S convection and surface wind deviation composites are similar to each other, both having large-scale deviations of both enhanced and reduced convection. The enhanced convection in the case WARM composite extends further into the eastern Pacific and has its peak amplitude later than the case REGULAR composite. In both composites, the reduced convection occurs over the Maritime Continent and peaks in the days following the center day. The surface wind and enhanced convection deviations in both cases are similar, showing an eastward translation somewhere between 5 and 8 ms^{-1}. This translation speed is larger than that discussed in Chapter II, who found a translation between 3-4 ms^{-1} for the Type S WWE. The Chapter II composite analysis did not treat the case REGULAR and WARM composites separately. In the case REGULAR composite, the enhanced convection is evident on Day (-9) in the equatorial western Pacific, and reaches the dateline by the center day, with the enhancement concentrated south of the equator. In the case WARM composite, the enhanced convection is evident as early as Day (-6), increasing in amplitude and extent through Day (3) by when it extends far past the dateline in the southern hemisphere.

viii) TYPE SE (FIGURE IV.16):

The case REGULAR and WARM Type SE composites are similar to each other. The main difference between the two is that the case REGULAR Type SE composite has wind deviations throughout the basin, while the case WARM composite has sparser areas of significance. The main convective patterns in both composites are enhanced convection near the main surface wind deviations in the classifying region, and a region of reduced convection extending to the southeast from the Maritime Continent to the dateline near 30°S.

The surface wind deviations in the case REGULAR composite are evident in the

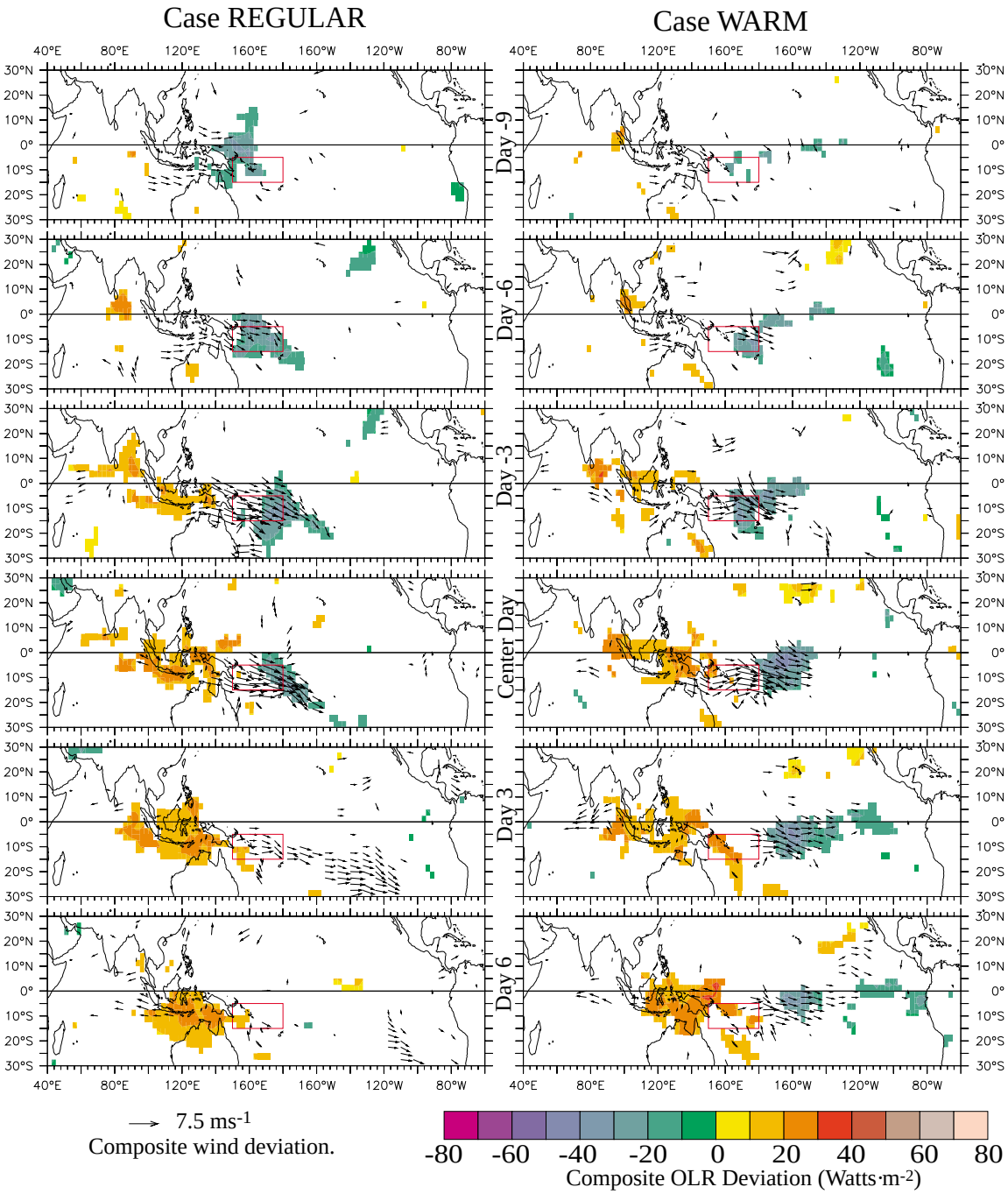

Figure IV.15: Composite evolution of the Type S OLRD and **UD** fields for (left column) Case REGULAR, (right column) Case WARM. Composite goes from Day (-9) though Day (6) by 3 day intervals. Shaded is OLRD, with cool (warm) colors indicating enhanced (reduced) convection, masked at the 99% confidence level. Wind deviation vectors are plotted if either the zonal or meridional component is significant at the 99% confidence level.

northern hemisphere western Pacific (near the Type NW classifying region) by Day (-9). The surface westerlies appear in the Type SE classifying region following Day (-6); developing a cyclonic circulation structure near the center day. There are equatorial westerlies in the case REGULAR composite. It appears that both the co-occurrence between the Type NW and SE events and the composite equatorial westerlies associated with the Type SE WWE mentioned in HV97 and Chapter II, result from the evolution of the Type SE events when NIÑO3 SST is near normal.

The surface wind deviations in the case WARM composite appear west of the Type SE classifying region by Day (-9) and intensify. By the center day the winds have developed a cyclonic circulation structure. By Day (6) the only large-scale deviations remaining are reduced convection north of New Guinea and to the south of the classifying region.

ix) SUMMARY:

The convective variability associated with each WWE type is complex, and not generally suggestive of a tight association between the WWE types and particular atmospheric circulation phenomena (*ie.* the MJO, tropical cyclones, convective superclusters, etc.). The composites of the Type NW and W WWEs are suggestive of an association between these WWE types and tropical cyclone activity. The eastward propagation seen in the Type S and SE composites, is consistent of a relationship between these event types and both the MJO and tropical cyclone activity (since tropical cyclones in that part of the world generally translate southeastward at ~3-5 ms^{-1}). The propagation speed of these southern hemisphere WWEs is consistent with both the typical translation of southern hemisphere tropical cyclones and with the phase speed MJO convective variability (although not with the phase speed of MJO tropospheric wind variability).

The connection between convection in general and surface westerlies is clear from these composites; yet further analysis is necessary to understand the relationship between WWEs and circulation structures such as the MJO or cyclones. The fact that individual

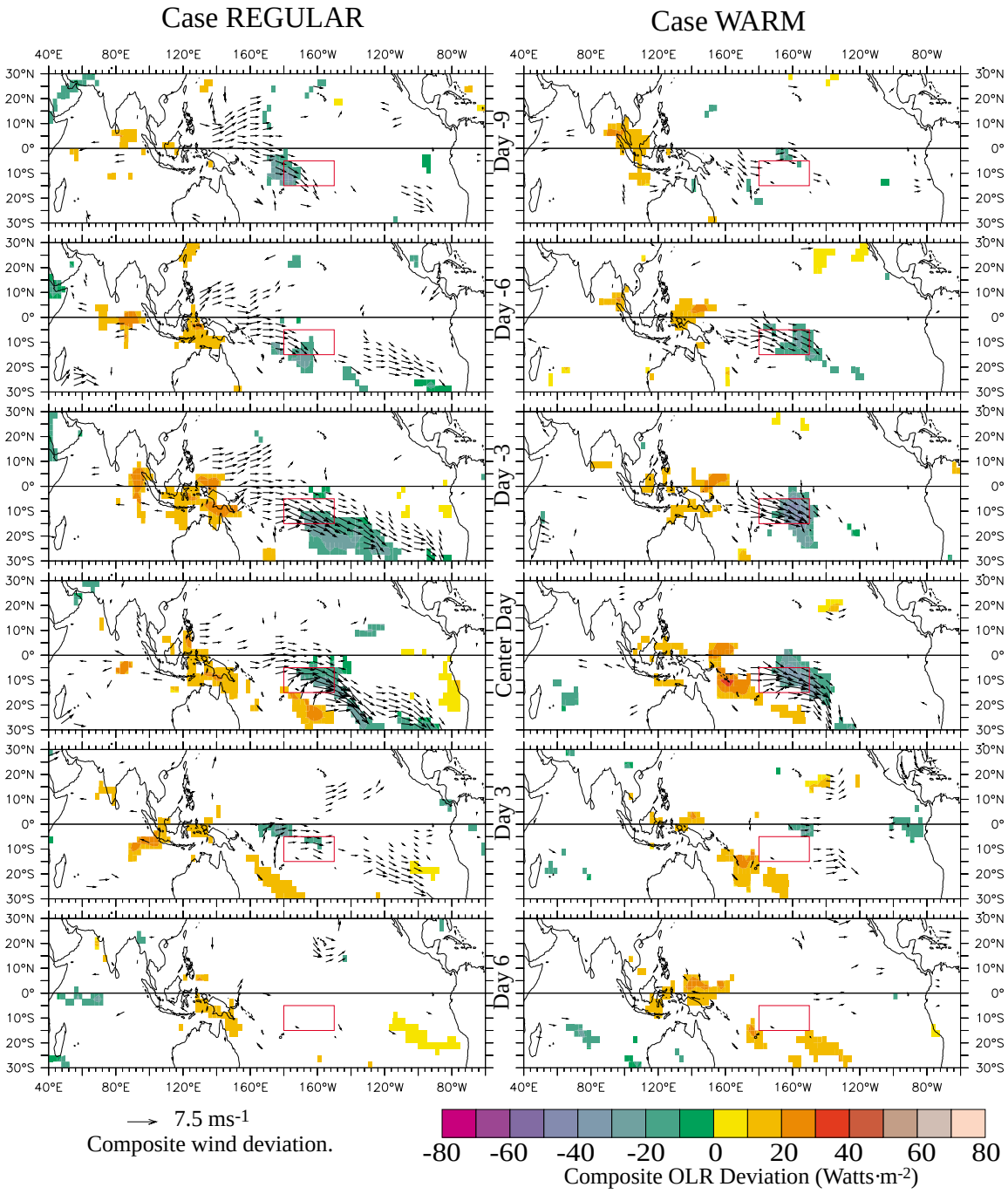

Figure IV.16: Composite evolution of the Type SE OLRD and **UD** fields for (left column) Case REGULAR, (right column) Case WARM. Composite goes from Day (-9) though Day (6) by 3 day intervals. Shaded is OLRD, with cool (warm) colors indicating enhanced (reduced) convection, masked at the 99% confidence level. Wind deviation vectors are plotted if either the zonal or meridional component is significant at the 99% confidence level.

WWEs have been observed with a variety of atmospheric circulation phenomena (mid-latitude cold surges, paired tropical cyclones, individual tropical cyclones, the convectively active phase of the MJO, convective superclusters, etc.) is consistent with the fact that no single circulation phenomenon appears clearly in the WWE composites. A general relationship between WWEs and any single mode of atmospheric variability cannot be developed from these results. In the next section I examine the "inter-WWE" spacing to explore relationships between WWEs, and between WWEs and the MJO. In sections 5 and 6, I examine relationships between WWEs and these two particular circulation structures: the MJO (in Sections 5) and tropical cyclones (in Section 6).

IV.4. Inter-WWE Spacing:

Exploring the inter-WWE spacing gives an opportunity to understand the "randomness" of WWE occurrence and to explore suggestions of a tight coupling between WWEs and 40-80 day variability. The distribution of inter-WWE spacing can be tested for significant difference from an exponential distribution. If there are no significant departures, WWEs can be thought of as Poisson distributed random phenomena. If there are significant departures, the location of the departures can include hints as to the preferred timescale WWEs.

One of the fundamental features of the MJO, in fact the feature leading to its identification, is its strong spectral peak between 40 and 80 days. A phenomenon strongly associated with the MJO might be expected to have a spectral peak in the 40-80 day range. The duration of WWEs (typically 3-20 days, see Chapter II and HV97) is not consistent with the timescales of the MJO; yet it is possible that the MJO drives episodic variability with WWE timescales, with a typical spacing on the order of the MJO period. In this section, the spacing between successive WWEs of each type is examined to determine whether a suggestion for a relationship between the MJO and WWEs is evidenced in the inter-WWE spacing.

Figure IV.17 shows histograms for the spacing between successive WWEs of each

type for the period 1986-1998. The large bin size is 40 days, and the narrower bins are 10 days wide. Indicated on each 40 day bin is the 95% significant range expected from an exponential distribution with scale parameter fit to each WWE type. An exponential distribution has a probability density function given by:

And the maximum likelihood estimator for the exponential factor is the population average (Rice 1995, Zwillinger 1996). For each WWE type the exponential factor is approximated as the average days between WWEs, and a Montecarlo method is used to compute statistical significance (Rice 1995). The 95% confidence interval for the estimated exponential distribution is indicated by the vertical lines at the center of each bin. When the distribution

$$f(x) = \begin{cases} \lambda e^{-\lambda x} & x \geq 0 \\ 0 & x < 0 \end{cases}$$

is outside the 95% confidence interval in any bin, the distribution is significantly different from an exponential with the calculated factor at the 95% confidence interval.

All the WWEs have a peak in inter-event spacing in the -40 day range, roughly consistent with an exponential distribution. However, three WWE types (N, C and E) have significantly more WWEs occurring within 40 days of each other than expected from random. This spacing is consistent with the spectral character of the zonal wind near the dateline which has its largest sub-seasonal peak in the 6-30 day range (Luther *et al.* 1982, Harrison and Luther 1990). None of the event types deviate by having too many (or few) events in the 40-80 day bin.

Limiting the analysis to strong WWEs, the distribution of inter-event spacing is different for some event types. The inter-WWE spacing histograms for the events with zonal wind anomaly averaged over the classifying region exceeding 4 ms^{-1} is shown in Figure IV.18, with bins of 10 and 40 days width. It is clear from Figure IV.18, that the strongest southern hemisphere WWEs tended to be 40-80 days apart from each other. For the Type C and E strong WWEs, the strong event spacing is significantly different (at the

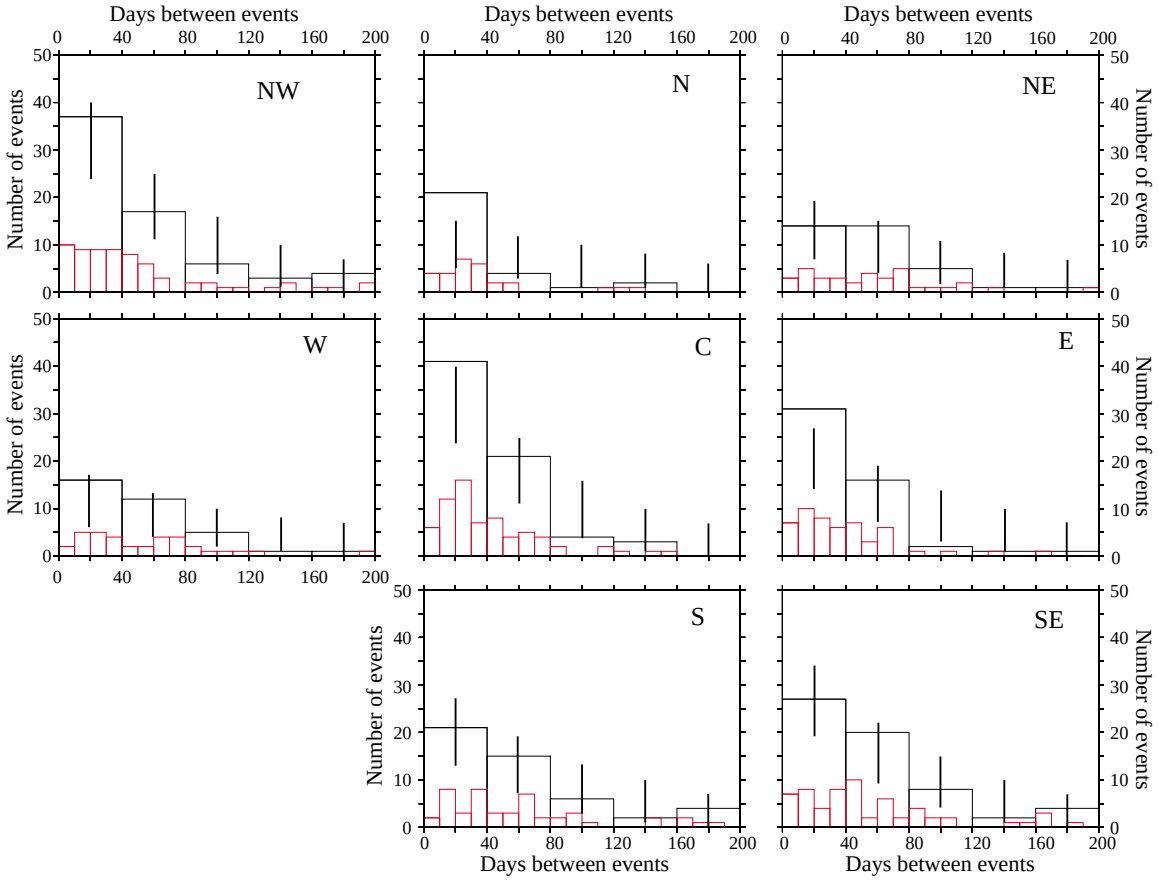

Figure IV.17: Histograms of the spacing between successive WWEs for each of the eight WWE types. Narrow bins are 10 days wide, wide bins are 40 days wide. Notice how no WWE type has a peak inter WWE spacing in the "intra-seasonal" 40-80 days band. Vertical lines indicate the 95% confidence interval for the distribution.

95% confidence level) from an exponential distribution. All other strong WWE types are indistinguishable from Poisson random phenomena.

The histograms shown in Figure IV.17 do not suggest a general relationship between WWEs and 40-80 day forcing. There are secondary peaks in that range for some WWE types, but the main inter-event spacing peak is ~40 days for all WWE types. The event spacing is for the Type C and E events is consistent with the spectral character of tropical Pacific zonal winds, which have about twice as much energy in the 6-30 day band as in the 30-90 day band (Harrison and Luther 1990). When only strong events are considered (Figure V.18), southern hemisphere WWEs (Types S and SE) have a prominent peak in the 40-80 day period. This spacing, along with the OLR and surface wind composites, is

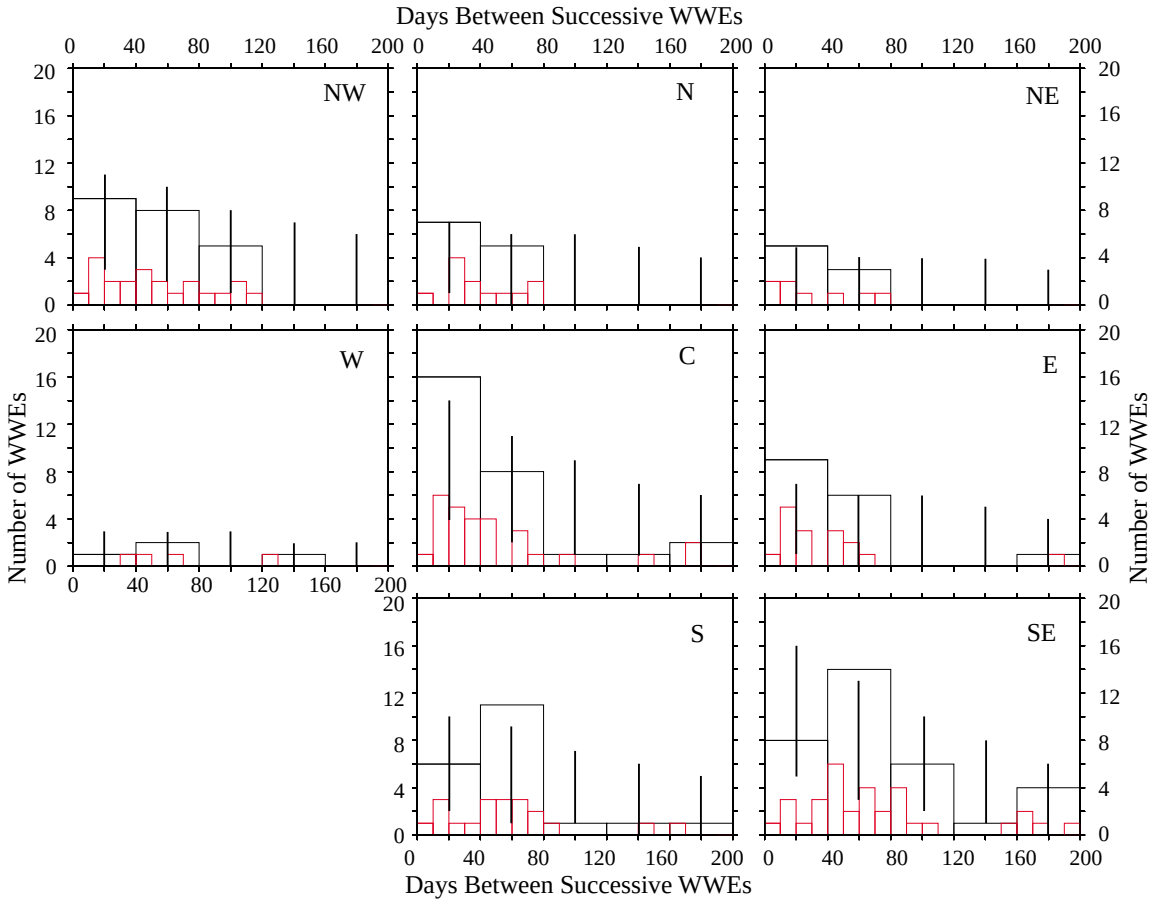

Figure IV.18: Histograms of spcaing between successive strong WWEs for each of the eight WWE types. "Strong" WWEs are those whose maximum zonal wind anomaly averaged over the classifying region exceeds 4 ms^{-1}. Narrow bins are 10 days wide, wide bins are 40 days wide. Notice how southern hemisphere WWEs have a peak in the "intra-seasonal" 40-80 day band, while no other WWE type has such a peak. Vertical lines indicate the 95% confidence interval for the distribution.

suggestive that the strongest southern hemisphere WWEs on record might be related to the MJO. In the next section, I use the MH98-MJOI to explore relationships between WWEs (as identified here) and the MJO (as defined by the MH98-MJOI).

IV.5. WWE/MJO co-occurrence.

In the previous section the inter-event spacing was explored to look for a suggestion of a systematic WWE/MJO relationship. In this section the search for WWE/MJO relationships is carried out using the MH98 MJO Index (MH-MJOI) and the WWE center day list. The MH-MJOI is an index derived independently from the WWE definitions, which uniquely

defines MJO events. These events are divided into 9 Phases, of which Phases 6-9 are the ones with enhanced western and central Pacific convection and surface westerlies (see Maloney and Hartmann 1998, Section 3). According to the MH-MJOI there were 70 MJO events in the period Jan 1986 through May 1998. If we use the NIÑO3 SSTA at the beginning of Phase 4 to separate the MJOs, we find that 20 (29%) occurred in case WARM, 44 (63%) occurred in case REGULAR and 6 (9%) occurred in case COOL; this distribution is not significantly different than a uniform distribution even at an 85% confidence level (see Table IV.1).

In this section, I first examine the distribution of WWEs relative to the Phases of the MJO, and perform two distinct tests of the distribution of WWEs into the MJO Phases. The first test examines whether the number of WWEs occurring when no MJO is present is significantly different from a binomial distribution, with probability given by (1-*p(MJO)*). This first test will determine whether a WWE is likelier to occur when an MJO is present than when it is not. The second test is whether, for the WWEs occurring inside the MJO, I am able to identify a sequence of Phases within which occur a preferential number of WWEs. If I am able to identify these Phases, they will then be referred to as the "WWE-rich" Phases of the MJO. Two combinations of the results occur in these data, and I interpret them as:

- *MJO modulation of WWE occurrence:* If a given WWE type has a distribution such that the number of WWEs occurring with the MJO is indistinguishable from random, but the events occurring within the MJO exhibit a preference for particular Phases of the MJO; then the MJO can be thought of as modulating the occurrence of WWEs. That is, WWEs are as likely to occur with an MJO as without, but if they happen with an MJO they tend to happen within certain Phases.

- *MJO driving of WWE occurrence*: If a given WWE type has a distribution that shows both a preference for the MJO and for particular Phases of the MJO, the distribution

is consistent with the WWEs occurring during the WWE-rich Phases of the MJO being driven by the MJO. This statistical relationship does not imply causality, but it is consistent with it.

Histograms of the MJO Phase at the beginning of the WWE for each WWE type are shown in Figure IV.19 (IV.19.a-.f, .h and .i), along with the distribution of the MJO phases over all time (IV.19.g). Notice, in Fig. IV.19.g, that about 34% of the time there are no MJOs present and the rest of the time is split pretty evenly among each MJO Phase; Phases 1 and 9 have less time in each of them because some MJOs occur in succession. Identification of the MJO Phases with an increased number of WWEs in them presents a problem in the easternmost regions, since the expected Phases roll over past Phase 9. For the easternmost WWE Types (NE, E and SE), histograms of the MJO Phase 5 days prior to the WWE beginning are shown in Figure IV.19 (shifting by 5 days was chosen because the average length of a Phase was 5 days; note that varying the shift between 5 and 10 days does not alter the principal results). Bars in the non-MJO bin of each WWE type indicate the limits of the 95% confidence interval for a binomial distribution with $p = 0.66$.

None of the WWE types has a statistically significant preference for MJO periods at the 95% confidence level. For the type W WWE, there is significant preference at the 90% level. For none of the other event types is the distribution distinguishable from a binomial even at the 85% confidence level.

The distribution for the various WWEs shows a peak in frequency of occurrence for most WWE types between Phases 6 through 9. This peak tends to move later in the MJO from the westernmost to the easternmost regions (notice the peak for Type W is Phases 6-8, and for Type C it 7-9), this is consistent with the MJO's eastward propagation of 40° longitude per Phase. (360° longitude / 9 Phases). By examining the distribution of MJO Phases for each WWE and performing bootstrap significance analysis on the co-occurrence statistics, a statistically significant "WWE-rich" Phases of the MJO can be defined for each

WWE type, where the number of WWEs occurring in the Phases is significantly different from a uniform distribution.

In Table IV.3 are listed, for each WWE type: the WWE-rich Phases of the MJO, and for all time and for each NIÑO3 SSTA state, the percentage of WWEs in the WWE-rich phases of the MJO. Highlighted by bolding are the statistics for which at least 50% of the WWEs occur in the WWE-rich phases of the MJO. For all time, only the Type W WWE has more than half its events occurring during the WWE-rich phases of the MJO, for the rest of the WWE types the values are between 36% and 45%. For none of the WWE Types is the percentage of WWEs occurring in any NIÑO3 SSTA state significantly different from the

Figure IV.19: Distribution of the MJO Phase in which a WWE begins, for each of the eight WWE types. Phases 1 through 9 refer to the Maloney and Hartman (1998) MJO definition, Phase 0 indicates that the WWE began when no MJO was identified. Bottom left panel shows the all time distribution of MJO phases. Notice how there are "WWE-rich" phases for most WWEs, coincident with the westerly phase of the MJO over the tropical Pacific. Stars indicate the lower limit of the 95% confidence interval of a binomial distribution for the non-MJO periods.

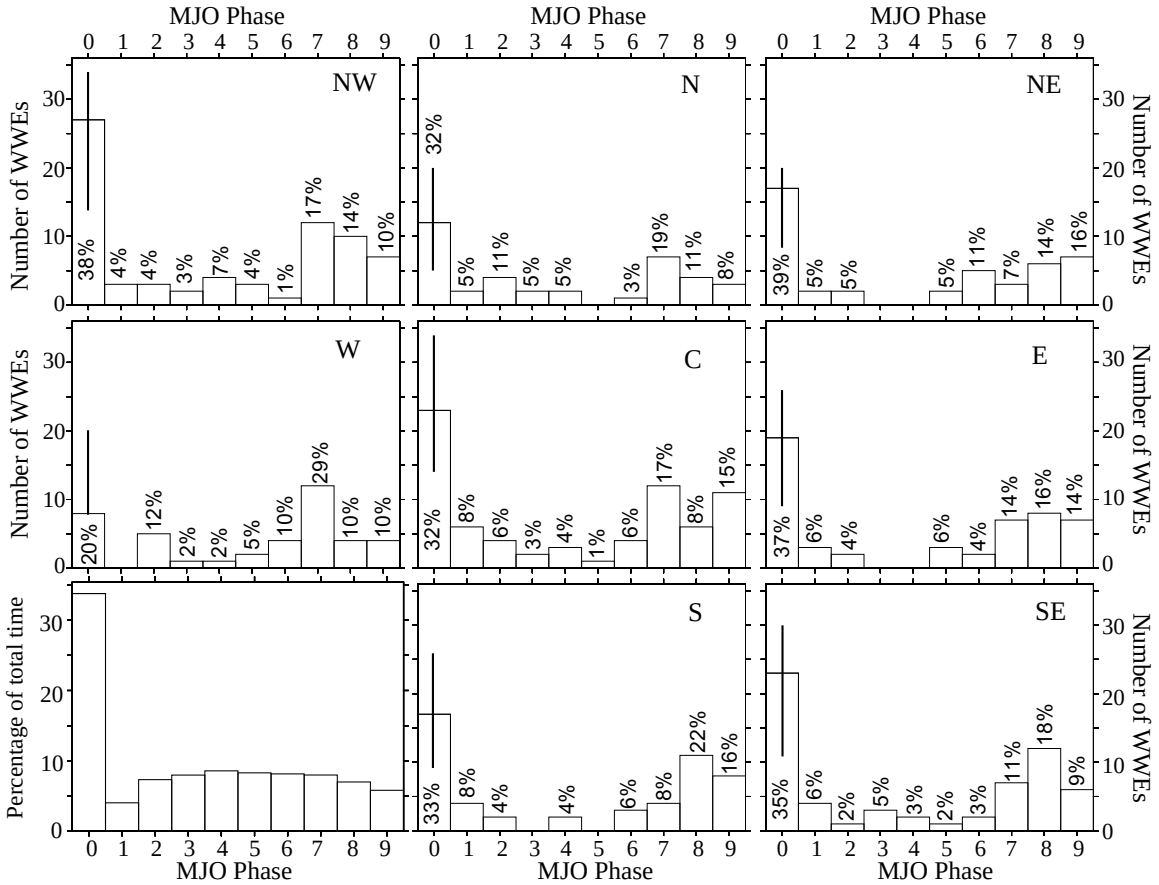

all-event case at the 95% confidence level.

Table IV.4 lists for each WWE type and for each NIÑO3 SSTA case: the percentage of MJOs which had a WWE occurring during the corresponding WWE-rich Phase. Also listed are the collective statistics for the northern hemisphere WWEs, equatorial WWEs, southern hemisphere WWEs, all WWEs, and for Type W and C WWEs (these particular WWEs are those most strongly associated with the onset and maintenance of warm El Niño SST anomaly changes; see VH00 and Chapter III). Percentages higher than 50% are highlighted by bolding.

The number of MJOs with any particular WWE occurring in the corresponding WWE-rich Phases is larger than what would be expected from random, yet over all time there is no individual WWE type which occurs in more than 50% of the MJO events. The highest percentage is for the Type NW WWE, which occurs in 39% of all MJO events. When WWEs are grouped together, the percentages increase, and when all WWEs are considered the percentage of MJOs with a WWE is close to 75%. It is common for MJO events to have a WWE during the corresponding WWE-rich Phases of the MJO, however it is not characteristic (as defined in Section IV.2) of the MJO.

Table IV.3: Percentage of westerly wind events beginning during the WWE-rich phases of the MJO, for the period Jan 1986 - May 1998. The statistics are computed for all time, and also separately for each NIÑO3 SSTA state (as defined in Section 2). The second column lists the WWE-rich phases of the MJO which correspond to each WWE type; for the easternmost WWE types the 5 day shifted statistics are computed (see text for discussion).

WWE Type	WWE-Rich MJO Phases	Percentage of WWEs beginning during WWE-rich phases			
		All Time	CaseWarm (NIÑ03 > 0.75ºC)	Case Regular (|NIÑ03| ≤ 0.75ºC)	Case Cool (NIÑ03 < –0.75ºC)
NW	7,8,9	40%	35%	44%	29%
N	7,8,9	38%	33%	39%	**50%**
NE	7,8,9 (SHF)	36%	24%	**50%**	20%
W	6,7,8	**51%**	36%	**57%**	
C	7,8,9	40%	37%	43%	
E	7,8,9 (SHF)	41%	37%	48%	
S	7,8,9	45%	44%	46%	40%
SE	7,8,9 (SHF)	41%	42%	40%	40%

Examining the distribution of MJOs with WWEs separately for each NIÑO3 SSTA state, a case REGULAR MJO is likelier to have a Type NW or N wind event than a case WARM MJO (at the 95% confidence level). For none of the other event types is the distribution within NIÑO3 SSTA states of WWE/MJO co-occurrence distinguishable from the distribution of the WWEs within NIÑO3 SSTA states.

MJO events have a significant co-occurrence with WWEs, when all WWEs are considered, 74% of MJO events have a WWE occurring during the WWE-rich phases. When only those events most strongly associated with the onset and maintenance of ENSO (Types W and C) are considered: between 47% and 60% of MJO events have WWEs of those types, and between 37% and 57% of those WWEs occur during the WWE-rich phases of the MJO.

Figure IV.20 shows a scatter plot of the NIÑO3 SSTA changes following an MJO, color coded by whether the MJO had an equatorial WWE during its "WWE-rich" phases.

Table IV.4: Percentage of MJO events with a westerly wind event beginning during the WWE-rich phases of the MJO, for the period Jan 1986 - May 1998. The statistics are computed for all time, and also separately based NIÑO3 SSTA state at the beginning of Phase 4 of the MJO. Percentages higher than 50% are hightlighted by bolding.

WWE Type	Percentage of MJOs with a WWE beginning during the WWE-rich phases			
	All Time	Case Warm (NIÑ03 > 0.75ºC)	Case Regular (|NIÑ03| ≤ 0.75ºC)	Case Cool (NIÑ03 < -0.75ºC)
NW	39%	25%	43%	**50%**
N	17%	15%	40%	
NE	21%	15%	25%	17%
W	23%	20%	27%	
C	37%	**60%**	32%	
E	29%	**55%**	20%	
S	33%	45%	30%	17%
SE	34%	**50%**	30%	17%
Northern Hemisphere	**54%**	45%	**57%**	**67%**
Type C or W	47%	**60%**	48%	
Equatorial	**54%**	**75%**	**52%**	
Southern Hemisphere	44%	**60%**	40%	17%
Any Type	**74%**	**80%**	**73%**	**67%**

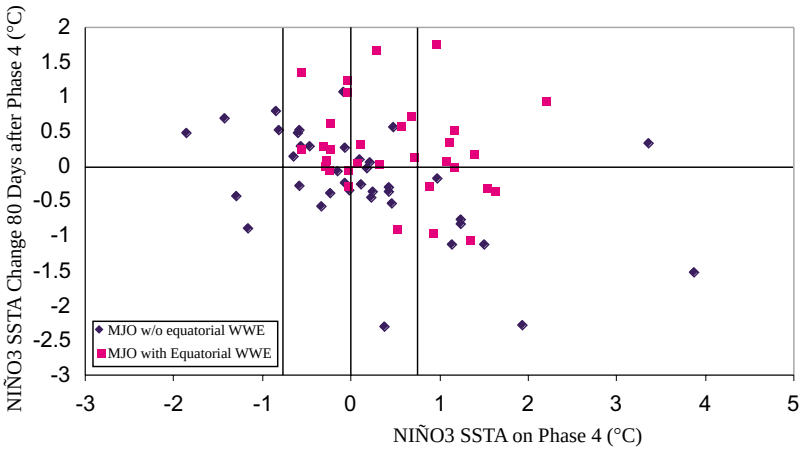

Figure IV.20: Scatter-plot of NIÑO3 SSTA Changes following MJO events. MJO events with equatorial WWEs during their "WWE-rich" Phases are hightlighted by pink squares. Note that the MJOs occurring with equatorial WWEs tend to be followed by warming, while those without WWEs tend not to be.

The NIÑO3 SSTA changes following MJOs in the absence of equatorial WWEs are not significantly different from the population as a whole. However, the SSTA changes following MJO events with an equatorial WWE in them is for significant warming when NIÑO3 SSTA is close to normal and for warm SSTA maintenance when NIÑO3 SSTA is warmer than normal. These expected changes are similar to those following equatorial WWEs. The expected NIÑO3 SSTA changes following MJOs are related to the presence (or absence) of equatorial WWEs.

I now examine the NIÑO3 SSTA changes following the equatorial WWEs, to determine if there is a significant difference between the changes following MJO related WWEs and other WWEs. One of the primary motivations for the study of WWEs has been their potential impact on the evolution of the El Niño cycle. In fact, in Chapter III and VH00, I show equatorial WWEs to be a fundamental mechanism in eastern Pacific SST warming prior to, and of warm SST maintenance during, El Niño. Figure IV.21 shows, for each equatorial WWE, scatter plots of NIÑO3 SSTA 20 days before the WWE center day vs. NIÑO3 SSTA change 60 days after the WWE center day (SSTA change is computed from Day(-20) SSTA), highlighting those WWEs which occurred during the WWE-rich phases of the MJO as stars. Vertical lines indicate the separation between the three NIÑO3 states

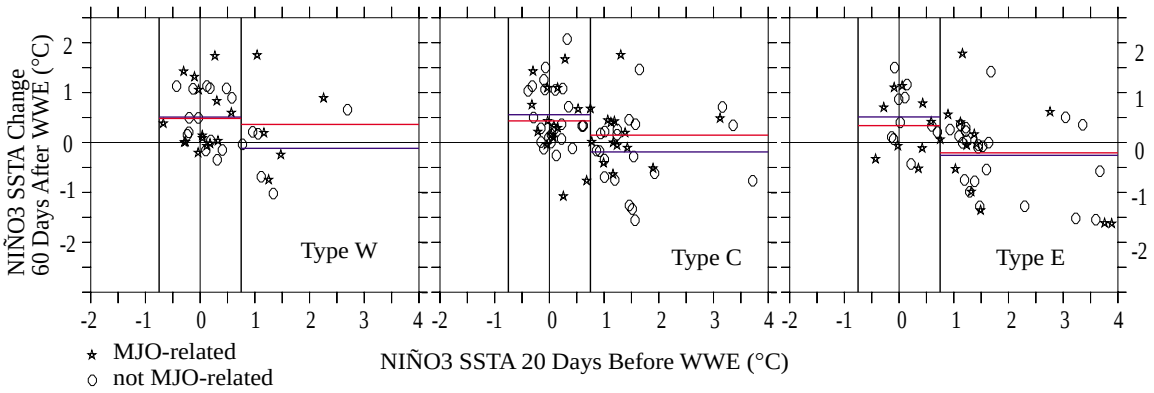

Figure IV.21: NIÑO3 SSTA Change 60 Days after a WWE vs. NIÑO3 SSTA 20 Days prior to the WWE for each of the three equatorial WWE Types. Data for those WWEs which occurred in the "WWE-rich" phase of an MJO are highlighted as stars. Vertical lines indicate the separation between the three NIÑO3 SSTA states (COLD, REGULAR and WARM). Red horizontal line indicates the mean for the MJO-related WWEs, blue horizontal line indicates the mean for the non-MJO-related WWEs. The means are not significantly different from each other.

(COOL, REGULAR and WARM), the red line indicates the mean NIÑO3 SSTA change within each state considering only those WWEs associated with the MJO, and the blue horizontal line in each of the states indicates the mean NIÑO3 SSTA change within each state considering only those WWEs not associated with the MJO.

Testing for significance using a Normal-*z* test at the 95% confidence level, I find that there is no significant difference in the mean SSTA change whether the event happened in association with the MJO or not, for any of the equatorial WWE types. When the eastern equatorial Pacific SST is warmer than normal, the mean SSTA change following MJO related WWEs is nominally larger than that following non-MJO WWEs, yet the difference is not significant (The difference in the Type W scatter plot appears large, but is not significant due to the small number of realizations). When the eastern equatorial Pacific SST is close to normal the mean SSTA change following non-MJO WWEs is nominally larger than that following MJO related WWEs, yet the difference is not significantly different from zero at the 95% confidence level. As far as warming of SST and maintenance of warm SST in the eastern Pacific during El Niño, MJO related WWEs are no different than non-MJO WWEs.

IV.6. WWE/Tropical Cyclone co-occurrence.

In this section, relationships between tropical cyclone activity and WWEs are explored. The co-occurrence statistics between WWEs and tropical cyclones in the respective regions of interest (as defined in Section 2 and Table IV.2) are summarized in Tables IV.5 and IV.6. Table IV.5 lists, for each WWE type, and for each NIÑO3 SSTA state: the percentage of WWEs for which a tropical cyclone is in the region of interest during the lifetime of the WWE, and the number of tropical cyclones in each region of interest. Table IV.6 lists, for each WWE type, and for each NIÑO3 SSTA state, the percentage of those cyclones which occurred during the lifetime of a WWE.

From the all event statistics in Table IV.5, one can see that this relationship between tropical cyclones and WWEs is strongest for the westernmost WWE types (NW and W), and weakest for the easternmost WWE types (NE, E and SE). Moreover, for the Type NE WWE the co-occurrence with tropical cyclones is not statistically significant even at the 90% confidence level. The relationship is *characteristic* (as defined in Section 2) for westernmost WWE types (NW and W); these statistics are consistent with the strong evidence for such a relationship in the surface wind and OLR composites. A majority (>60%) of the WWEs of each of the three types which are just west of the dateline (N, C and S) have

Table 5: Percentage of WWEs with a tropical cyclone in their respective region of interest during the lifetime of the WWE. The regions of interest are defined in Table 2. The statistics are broken down by NIÑO3 SSTA state on Day(-20) of the WWE.

WWE Type	**Percentage of WWEs co-occurring with a Tropical Cyclone**			
	All Time	Case Warm (NIÑ03 > 0.75ºC)	Case Regular (|NIÑ03| ≤ 0.75ºC)	Case Cool (NIÑ03 < -0.75ºC)
NW	86%	94%	88%	50%
N	62%	67%	65%	
NE	5%	9%		
W	90%	91%	90%	N/A
C	61%	62%	61%	N/A
E	26%	10%	35%	N/A
S	60%	68%	50%	80%
SE	38%	53%	21%	40%

a tropical cyclone occurring during the event lifetime. Even though the Type E and SE WWEs have a statistically significant relationship with tropical cyclones (at the 95% level), neither of these types has more WWEs occurring with cyclones than without.

Examining each NIÑO3 SSTA state separately in Table IV.5 and testing at the 95% confidence level, the percentage of WWEs associated with cyclones when NIÑO3 SST is close to normal is not significantly different than that when NIÑO3 SST is warmer than normal for the Type NW, N, W and C WWEs. For Types S and SE, there is a significantly greater number of WWEs associated with cyclones when NIÑO3 SST is warmer than normal than when it is close to normal. The WARM state enhanced relationship between cyclones and WWEs is especially prominent for the Type SE WWE, where a majority of case WARM events are associated with cyclones. For the Type E WWE more events occur when NIÑO3 SST is close to normal than when it is warmer than normal; despite the fact that most cyclones in the Type E region of interest occur when NIÑO3 SSTA is warmer than normal. Again, due to the small number of realizations when the eastern Pacific is cooler than normal, the statistics are not significant.

I now examine the number of tropical cyclones which have a WWE related to them. These statistics indicate that, while WWEs are associated with cyclones, the converse is not true. Table IV.6 shows that generally only 34-37% of tropical cyclones occur during a WWE (Type W has 20% and Type S has 43%; the Type NE statistics are not significant at the 95% level). These statistics are all significant at the 95% confidence level (except for Type NE), but in no region do a majority of cyclones co-occur with WWEs. When only cyclones of larger intensity are considered, the statistics for some WWE types become stronger: 54% of Typhoons (out of 46) and 58% of Category 2 Typhoons (out of 26) in the Type C region of interest occur during the lifetime of a Type C WWE, and 50% of Category 2 Hurricanes (out of 12) in the Type SE region of interest occur during the lifetime of a Type SE WWE. However, neither of these statistics gives an overwhelming percentage of cyclones (or ty-

phoons/hurricanes) co-occurring with WWEs. When the different NIÑO3 states are examined separately one finds that most WWE types have a higher cyclones/WWE co-occurrence when the eastern Pacific is warmer than normal that when it is cooler than normal; the exception being Type W event.

Occurring with a cyclone is a characteristic feature of the Type NW and W WWEs. However, most cyclones in the Type NW and W regions of interest are not associated with a WWE. Most west-of-dateline WWEs are associated with cyclone formation, and very few east-of-dateline WWEs are associated with cyclone formation. The WWE-cyclone association for west-of-dateline WWEs is stronger than the WWE-MJO association. For east-of-dateline WWEs the WWE-MJO association is as strong or stronger than the WWE-cyclone association.

IV.7. Summary and Discussion.

In this chapter I computed the surface wind and convective structures associated with the MJO (Section IV.3.a) and WWEs (Section IV.3.b), described statistical relationships which WWEs exhibit with the MJO and tropical cyclones, and examined the inter-WWE spacing statistics for the period 1986-1998. WWEs are generally convective events

Table 6: Characteristics of the cyclones which occurr in the regions of interest of each WWE type. Columns 2 through 5 list the percentage of tropical cyclones in each region of interest which co-occurr with the respective WWE type.

WWE Type	Percentage of Tropical Cyclones co-occurring with a WWE			
	All Time	Case Warm (NIÑ03 > 0.75ºC)	Case Regular (|NIÑ03| ≤ 0.75ºC)	Case Cool (NIÑ03 < –0.75ºC)
NW	37%	47%	36%	13%
N	35%	58%	25%	
NE	13%		17%	
W	20%	20%	21%	15%
C	34%	51%	27%	
E	34%	53%	10%	
S	43%	43%	42%	75%
SE	37%	57%	21%	25%

which do not show much similarity to any individual convective mode of variability. The northwestern-most WWE Types (NW, N and W) are associated with tight convective structures suggestive of a tropical cyclone. Southern hemisphere WWEs are associated with eastward propagating convection near the main wind anomalies. Type C and E WWEs are associated with enhanced convection near the main equatorial westerly anomlies. The MJO is associated with equatorial surface wind anomalies across the entire tropical Pacific. WWEs appear to be modulated by the MJO; west-of-dateline WWEs show a stronger association with tropical cyclone activity than with the MJO.

I computed the convective and surface wind anomaly fields associated with the MJO using a compositing technique based on the Maloney and Hartmann (1998, MH98) MJO identification scheme (see Section IV.3.a). The convective structures identified by this compositing technique very much resemble those previously described in the literature in association with the MJO (*e.g.* Madden and Julian 1994, Rui and Wang 1994, Hendon and Salby 1994): there is an eastward propagating couplet of reduced and enhanced convection over the Indian Ocean and the western Pacific warm pool region. The convective structures propagate eastward at an average speed of ~5 ms^{-1} (based on the mean 5 day Phase length), which is in agreement with previous estimates (Madden and Julian 1994, Rui and Wang 1994, Hendon and Salby 1994). The agreement of the tropospheric circulation patterns described by MH98 and the convective structures described here, with the circulation and convective structures described in previous work gives confidence that the surface wind structures evaluated in the composite are representative of the MJO related surface wind variability.

The surface wind anomaly fields in the MJO composite (Figures IV.3-.5) do not much resemble recent idealizations of the MJO related surface wind variability over the tropical Pacific (Kessler *et al.* 1995, Kessler and Kleeman 2000). Kessler *et al*. (1995) and Kessler and Kleeman (2000) idealize the MJO surface expression based on the observed

convective variability associated with the MJO, which tends to be confined to the warm pool of the western Pacific Ocean. I find that near-equatorial Pacific surface wind anomalies extend beyond the western Pacific warm pool into the central and eastern Pacific. The amplitude of the eastern Pacific variability is smaller than that in the western Pacific, but since the eastern/central equatorial Pacific is dominated by strong and persistent easterly trade winds, the central/eastern Pacific momentum flux (surface stress) might not be negligible. I explore the equatorial Pacific SSTA variability driven by the composite MJO in an OGCM in Chapter V.

The relationship between most WWEs and the MJO appears to be that of the MJO modulating the occurrence of the WWEs within an MJO. For each WWE Type there I am able to define "WWE-rich" phases of the MJO, wherein the number of WWEs occurring is statistically significant, for only one WWE type do the majority of events occur in the "WWE-rich" Phases of the MJO (51% for the Type W WWE). However, one can also define a set of "WWE-poor" Phases of the MJO within which the number of WWEs occurring is significantly lower than expected, these Phases correspond to the convectively suppressed Phases of the MJO. These relationships are not surprising, since WWEs are associated with atmospheric convection (Section 3, Meehl *et al.*, 1995, Kiladis *et al.* 1994), the reduction and enhancement of convection associated with the MJO should be expected to modify WWE distribution. For most WWE Types the convective variability related to the MJO redistributes the probability distribution of WWEs towards the convectively active Phases and away from the convectively suppressed Phases.

There is a weakly significant idication (at the 90% level only) that relationship between Type W WWEs and the MJO is such that MJOs appear to enhance the occurrence of WWEs. This relationship might be due to the enhanced tropical cyclone activity related to the MJO (Liebmann *et al.* 1994), due to an enhancement of westerly wind variability related to the MJO directly, or is might be spurious. Note that the statistical significance of the

relationship between the MJO and Type W WWEs is not robust due to the small number of WWEs, having one more event occurring in the absence of the MJO would reduce the confidence below the 90% level. As the datasets expand in the future, the nature of the statistical relationship should be re-examined.

In examining the NIÑO3 SSTA changes following the MJO, I find that in the absence of equatorial WWEs there is no significant warming (or warm SSTA maintenance) following the MJO (see Figure IV.20). Following MJO events with equatorial WWEs, there is a tendency for NIÑO3 SSTA warming (or warm SSTA maintenance) of a similar character to that following equatorial WWEs (see Figure IV.21). Also, the expected NIÑO3 SSTA changes following equatorial WWEs are independent of their relationship to the MJO (see Figure IV.21). In Chapter V I examine OGCM response to composite MJO and WWE forcing to explore the dynamical aspects of Pacific waveguide SSTA changes following the MJO and WWEs.

In Chapter III and VH00, it was shown that equatorial WWEs are associated with the onset and maintenance of El Niño warming; the global MJO has no significant relationship with El Niño (see Figure IV.2, Table IV.1, Slingo *et al.* 1999, Hendon *et al.* 2000, Harrison and Vecchi 2000). The expected NIÑO3 SSTA changes following equatorial WWEs are independent of whether the WWEs occurred with an MJO or not (see Figure IV.19). Since WWEs are strongly associated with El Niño warming and mechanisms based on the observed surface wind structure of WWEs have been suggested to explain that link (Harrison and Giese 1988, Giese and Harrison 1990,1991, Chapter V), since the MJO shows no significant relation to El Niño, and since WWEs are related to NIÑO3 SSTA warming independent of the relation to the MJO: the connection between surface warming and WWEs seems stronger than with the MJO.

Examining the convective structures associated with WWEs (Section IV.3.b), I find that WWEs are generally associated with convection during the lifetime of the event. The

convective and wind structures of the western-most WWE Types (NW and W) are suggestive of a strong link between these events Types and tropical cyclone activity. This suggested association is confirmed in the WWE/cyclone co-occurrence statistics described in Section IV.6. Over 90% of Type NW and W WWEs are associated with tropical cyclone activity. Further, the relationship between west-of-dateline WWEs and tropical cyclone activity is always stronger than that between the MJO of WWEs.

WWEs and MJOs represent different aspects of tropical Pacific atmospheric variability, both with strong signals in atmospheric convection. The MJO appears to modulate the occurrence of WWEs in the intra-seasonal time-scale; however, the eastern Pacific SSTA changes following equatorial WWEs are independent of their relation to the MJO. Because WWEs are not related to any single atmospheric circulation phenomenon, and because WWEs are strongly linked with El Niño warming and maintenance, improved understanding and prediction of El Niño SSTA changes likely depends on better understanding and prediction of the entire range of atmospheric variability which brings about WWEs. This variability includes paired and individual tropical cyclones, the MJO, mid-latitude cold surges and convective superclusters.